Direct photon and charged hadron azimuthal correlation for the study of parton energy loss at top RHIC energy in STAR experiment

(Analysis Note)

PAs:
Ahmed Hamed, Saskia Mioduszewski, Nihar Ranjan Sahoo

September 15, 2015

Abstract

High energy heavy-ion collisions provide sufficient conditions for the formation of a deconfined plasma of quark and gluons (QGP). The direct-photon (γ^{dir}), those produced during the collision rather than from decays of hadrons, tagged away-side jet is proposed as a golden probe for studying the parton energy loss while traversing through the medium. We report the results of γ^{dir}+hadron and π^0+hadron azimuthal correlations for the measurement of the away-side jet yields in $0-10\%$ central Au+Au and p+p collisions at $\sqrt{s}_{\rm NN}$= 200 GeV in the STAR experiment. The charged-particle yields at midrapidity ($|\eta| < 1$) and transverse momentum (1.2 $< p_T^{assoc}$ GeV/c) associated with γ^{dir} and π^0 ($|\eta|$ <0.9, 12 $< p_T^{trig} <$ 20 GeV/c) are compared with p + p collisions. We observe same z_T dependence of suppression of the away-side associated charged particles in central Au+Au collisons as compared with that of p+p for γ^{dir} and π^0 trigger, within uncertainties. The supression of away-side charged hadrons per γ^{dir} trigger is independent of p_T^{trig} , whereas that show strong dependence on p_T^{assoc}. Finally, we compare our experimental measurements with existing theoretical models.

Paper Webpage:
http://www.star.bnl.gov/protected/jetcorr/nihar/PaperProposal/mainpage.html

Contents

0.1 Motivation

- The γ^{dir}-jet coincidence measurements have long been proposed as a golden probe for studying parton energy loss in the QGP medium [1]
- The outgoing high-pT γ^{dir} approximates that of initial partner parton p_T by π in azimuth ("away-side")
- High-p_T suppression at away-side γ^{dir}-jet events can give information about dense medium created in high energy heavy-ion collisions
- In addition, the mean-free path of the γ^{dir}in the medium is large enough, regardless of the position of the initial scattering vertex, compare with that of π^0. Hence the away-side parton associated with π^0 loses more energy on average than that associated with γ^{dir}
- A comparison between the spectra of the away-side particles associated with γ^{dir} vs π^0 triggers can give opportunity for the path length dependence study of energy loss of the partner parton
- The comparison between away-side parton associated with γ^{dir} vs π^0 triggers may give information about color factor dependence on energy loss

Therefore, γ^{dir} vs π^0 tagged charged hadron (fragmentation from partner parton) azimuthal correlation can provide suitable opportunity in the experiment to study the medium modification (I_{AA}) in AuAu collisions as compare with pp collisions.

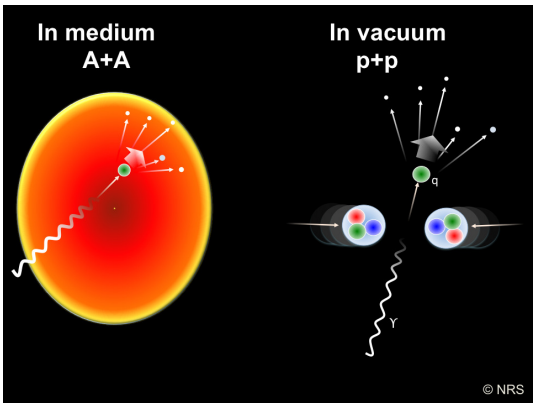

Published STAR experiment results [2] suggest that

- The dependence of I_{AA} (γ^{dir}-$h^{\pm}$) on p_T^{trig} shows no significant dependence on the initial parton energy within kinematic region $0.4 < z_T < 0.9$
- I_{AA} of γ^{dir}-$h^{\pm}$ shows no z_T dependence within $0.3 < zT < 0.9$

Hence, we investigate on the behavior of nuclear modification factor at low z_T by triggering high p_T ($12 < p_T^{trig} < 20$ GeV/c) γ^{dir} and π^0, and low p_T associated hadron ($1.2 < p_T^{assoc}$ (GeV/c))

0.2 Data sets and analysis details

Run-2011 Au+Au and Run-2009 p+p 200 GeV data sets are used for the direct photon and charged hadron azimuthal analysis. Here are the queries for FileCatalog :

Run-9 p+p 200 GeV:

get_file_list.pl -keys 'path,filename' -cond
'trgsetupname=commission2009_200Gev_Hi||
production2009_200Gev_Hi||
production2009_200Gev_noendcap||
production2009_200Gev_Single||tof_production2009_single,
production=P11id,filetype=daq_reco_MuDst,
filename~st_gamma,storage!=HPSS' -limit 0

Run-2011 Au+Au 200 GeV:

get_file_list.pl -keys 'path,filename' -cond
'trgsetupname=AuAu200_production_2011,
production=P11id,filetype=daq_reco_MuDst,
filename~ st_gamma,storage!=HPSS' -limit 0

Total ~1.8M and ~0.5M (0-10%) central events within $|V_z|$ <55 cm and $|V_r|$<2 cm, from L2Gamma trigger (Detail discussion on L2Gamma Trigger can be found at Ref [6]) for pp Run9 [5] and AuAu Run11 [4], respectively, have been analyzed after QA. Some bad runs are removed after removal of hot towers, η and ϕ strips in BSMD. The following plots show some event-QA for AuAu and pp collisions.

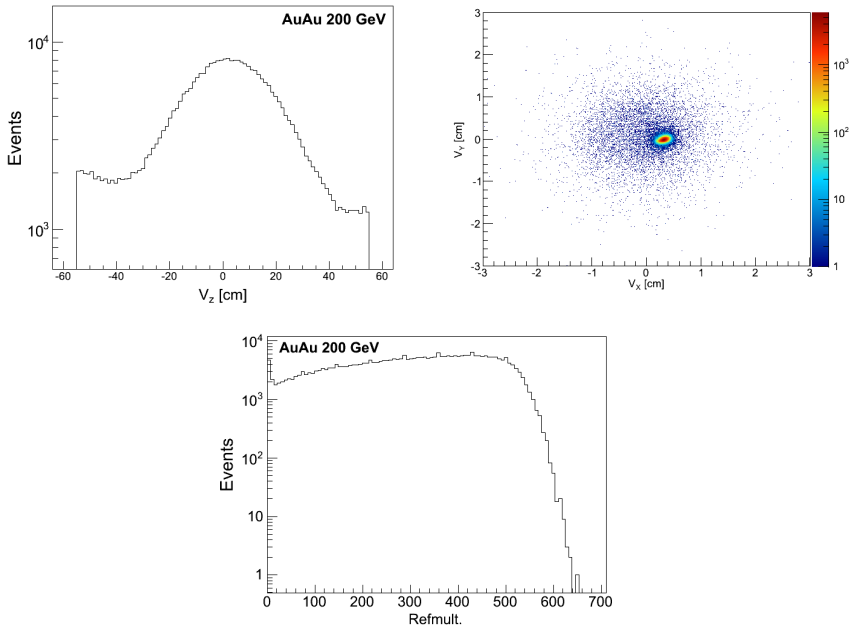

Figure 1: V_z, V_r and Refmult distributions for AuAu collisions.

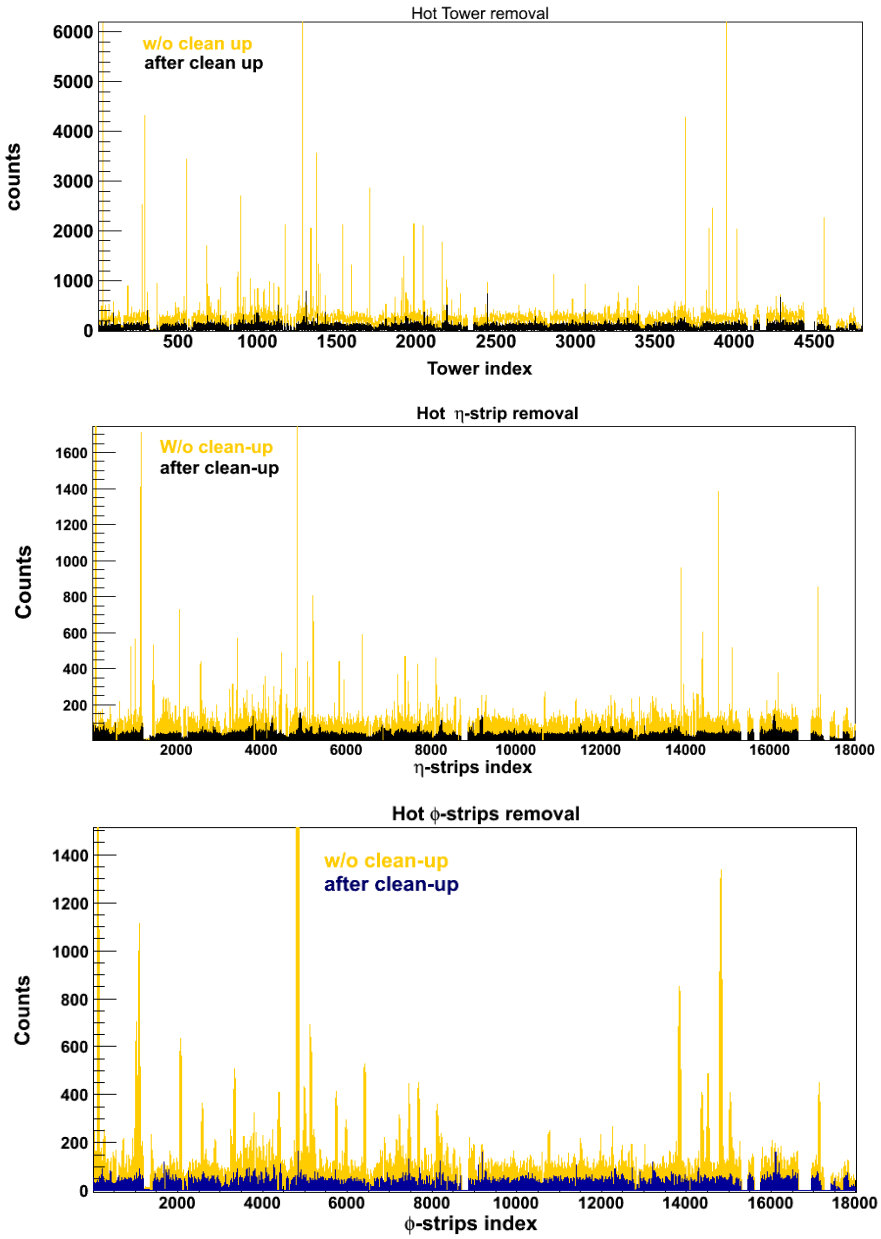

Figure 2: QA plots for hot towers, eta and phi strips for AuAu Run11. The yellow and dark bars represent before and after, respectively, hot towers and strips removal.

The TPC track quality cuts and charged hadrons selections (both for AuAu and pp) are listed below:

- $|\eta|$ <1.0
- 1.2<p_T^{assoc}<20.0 (GeV/c)
- Fit. Points > 15
- Track quality cut > 0.52
- dE/dx != 0
- DCA < 3 cm

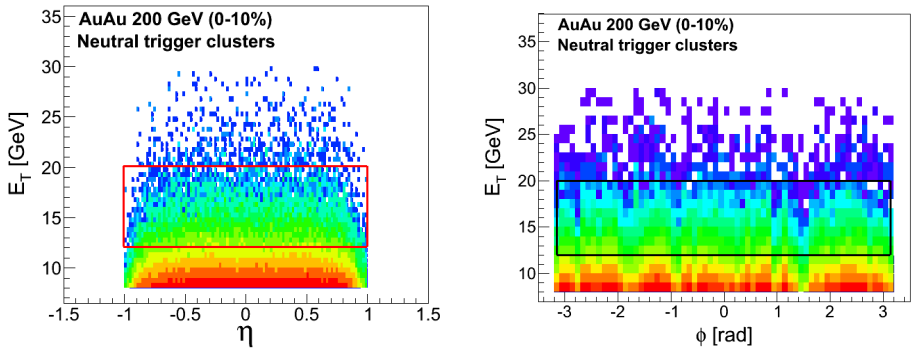

Figure 3: E_T vs. η and ϕ for AuAu collisions for neutral trigger clusters.

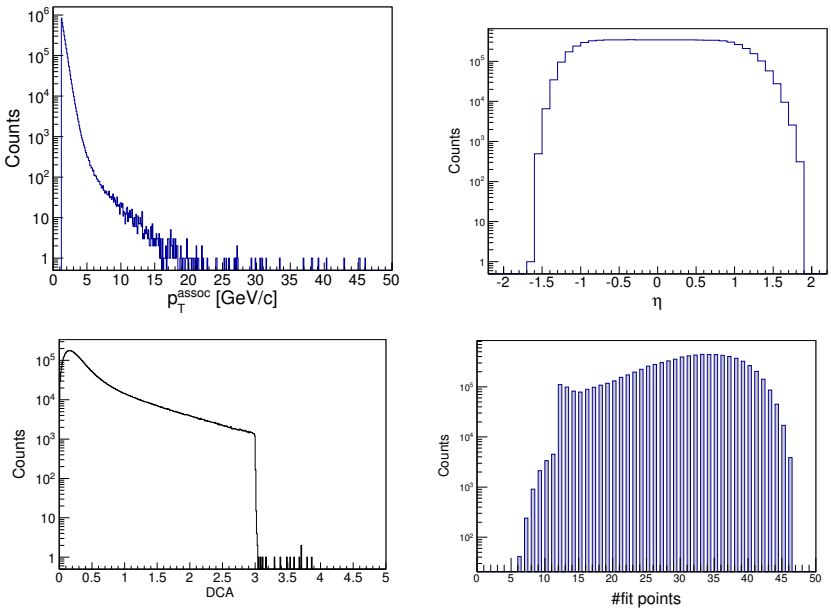

Figure 4: QA plots for TPC tracks for AuAu Run9.

The BEMC cuts (both for AuAu and pp) are listed below:

- E_T > 8 GeV
- Trigger tower rejected, if track having p > 3 GeV pointing towards it

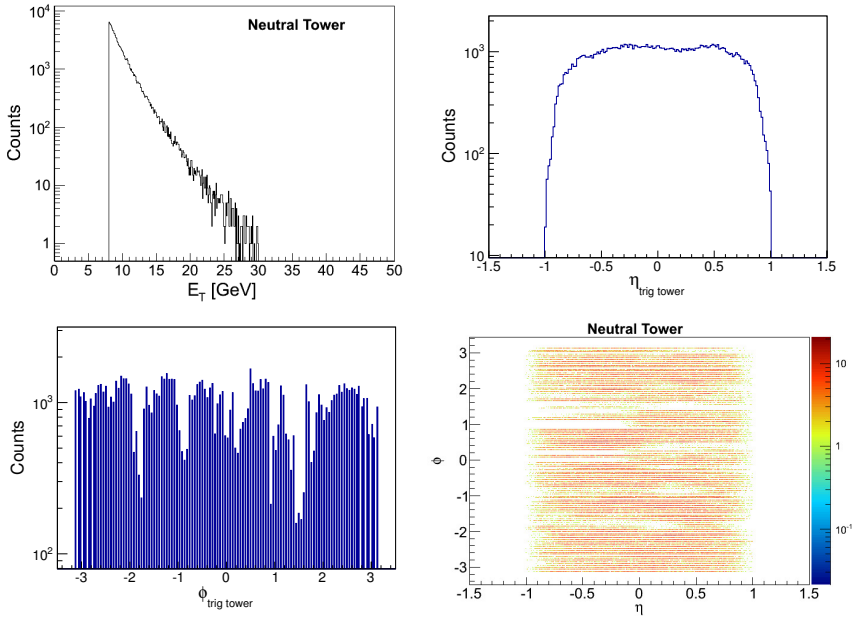

Figure 5: QA plots for BSMD for AuAu Run9.

- SMDeta > 0.5 GeV and SMDphi > 0.5 GeV
- $|\eta| < 0.9$
- $12 < p_T^{assoc} < 20$ GeV

Runlist used for this analysis for AuAu run11 st_gamma stream data sets

12170020, 12156032, 12149050, 12160022, 12149028, 12162042, 12155007, 12149048, 12167049, 12137024, 12151045, 12158059, 12164042, 12134055, 12151001, 12171008, 12163007, 12155062, 12162010, 12128020, 12169059, 12154043, 12167005, 12163021, 12170014, 12169062, 12132067, 12163002, 12158016, 12162014, 12157012, 12157046, 12171009, 12127023, 12160023, 12164044, 12164041, 12164008, 12137040, 12155015, 12163049, 12157052, 12156005, 12157039, 12157043, 12135051, 12153012, 12161009, 12170046, 12163057, 12162007, 12155040, 12165042, 12137021, 12157048, 12156056, 12159039, 12135024, 12163020, 12151062, 12151061, 12170012, 12170058, 12170027, 12171002, 12166059, 12156048, 12137035, 12137029, 12137026, 12167052, 12156030, 12128010, 12135057, 12135049, 12158005, 12169014, 12155029, 12149044, 12162011, 12133018, 12137012, 12163018, 12133052, 12134062, 12146004, 1215602912169052, 12165020, 12164040, 12164085, 12155057, 12169019, 12171012, 12150037, 12161052, 12164066, 12154038, 12164067, 12170056, 12164086, 12164053, 12164088, 12136007, 12138022, 12157024, 12138009, 12136050, 12136044, 12137023, 12156035, 12162059, 12150040, 12163008, 12137009, 12166052, 12167003, 12160005, 12146006, 12165015, 12166009, 12170031, 12156061, 12165005, 12166051, 12166054, 12165021, 12159022, 12161032, 12168079, 12153009, 12164005, 12135036, 12151006, 12160025, 12164043, 12151067, 12169027, 12161057, 12149045, 12138005, 12165008, 12133026, 12156016, 12154067, 12151004, 12170049, 12153034, 12158066, 12133007, 12165004, 12151009, 12151010, 12149047, 12156008, 12165003, 12134002, 12134005, 12169017, 12162019, 12155046, 12169028, 12158021, 12135005, 12158072, 12157016, 12134064, 12134067, 12135004, 12157013, 12158011, 12136047, 12135034, 1216906012164058, 12162018, 12156021, 12136041, 12136040, 12135060, 12155060, 12155016, 12155012, 12161030, 12157044, 12163024, 12168010, 12157031, 12158004, 12133022, 12134065, 12170026, 12155045, 12161025, 12168009, 12156038, 12134048, 12156006, 12171003, 12164050, 12137006, 12159019, 12155004, 12151066, 12156049, 12158025, 12169065, 12132068, 12171011, 12167004, 12150038, 12135002, 12155009, 12155013, 12156041, 12151064, 12150011, 12155054, 12154047, 12161024, 12156060, 12151002, 12159026, 12135030, 12149046, 12156010, 12155001, 12132070, 12152016, 12152015, 12167021, 12170011, 12159006, 12135046, 12159023, 12160006, 12136071, 12166006, 12133028, 12133027, 12166058, 12135014, 12155031, 12169042, 12156045, 12156051, 12135022, 12150019, 12150015, 12150026, 12134007, 12152008, 12157030, 12150008, 12168060, 12155038, 12133011, 12165022, 12135008, 12135006, 12135009, 12138012, 12161006, 12159012, 12168006, 12165001, 12134058, 12149051, 12132021, 12168005, 12170047, 12156046, 12157003, 12149059, 12150020, 12136080, 12156037, 12127049, 12155064, 12163003, 12169050, 12169023, 12160012, 12169022, 12127024, 12127004, 12127006, 12127038, 12128007, 12127005, 12126091, 12170051, 12171001, 12163051, 12134044, 12167040, 12156009, 12151011, 12154015, 12134026, 12134035, 12133006, 12126087, 12166005, 12134041, 12150041, 12163056, 12151063, 12154045, 12158041, 12159021, 12135037, 12155018, 12155050, 12150009, 12135058, 12153032, 12153018, 12150035, 12134013, 12157015, 12165026, 12163009, 12162031, 12156042, 12156050, 12156047, 12128019, 12128029, 12128011, 12151033, 12135033, 12133057, 12160016, 12153008, 12126093, 12161017, 12157009, 12132061, 12132062, 12156011, 12156015, 12168003, 12166057, 12154020, 12165012, 12136043, 12155008, 12154065, 12155047, 12149060, 12156044, 12171014, 12171010, 12150050, 12151012, 12169047, 12169043, 12152012, 12169045, 12155037, 12152011, 12132034, 12163006, 12163050, 12163017, 12169057, 12132043, 12160013, 12132066, 12167026, 12171013, 12159020, 12135055, 12134056, 12164004, 12137043, 12164009, 12132053, 12155048, 12167012, 12169049, 12132045, 12170004, 12170003, 12155019, 12154044, 12161014, 12161026, 12157010, 12155020, 12165007, 12150001, 12162002, 12169016, 12150034, 12164002, 12169024, 12149040, 12157028, 12158026, 12133003, 12164003, 12165037, 12158003, 12165028, 12167045, 12160019, 12169058, 12168059, 12158029, 12136001, 12154001, 12156002, 12127034, 12127033, 12149058, 12135043, 12136079, 12156020, 12137003, 12137004, 12137013, 12137033, 12136045, 12136053, 12167009, 12133038, 12158020, 12166008, 12161050, 12136064, 12170018, 12137034, 12137028, 12169046, 12127007, 12169030, 12133002, 12157042, 12162003, 12156018, 12165014, 12163019, 12159005, 12161021, 12151017, 12170050, 12137025, 12163055, 12127048, 12170028, 12155043, 12149063, 12166004, 12162027, 12133056, 12160004, 12159018, 12169056, 12164056, 12161022, 12156003, 12158010, 12158019, 12127008, 12151005, 12137037, 12151013, 12169055, 12162045, 12136074, 12150013, 12150012, 12166061, 12133039, 12159024, 12154066, 12162029, 12134030, 12128001, 12136083, 12154003, 12154011, 12149062, 12170048, 12133019, 12133023, 12164057, 12134031, 12134016, 12161012, 12165023, 12127040, 12138007, 12156004, 12137039, 12150021, 12164010, 12164048, 12132024, 12154019, 12155051, 12155058, 12155055, 12149035, 12160021, 12150003, 12133041, 12153014, 12154008, 12167002, 12163010, 12155061, 12155065, 12154004, 12146008, 12158051, 12170013, 12136078, 12136070, 12170005, 12170002, 12167011, 12135010, 12135013, 12158009, 12170032, 12134028, 12134032, 12134033, 12134015, 12134012, 12151023, 12166010, 12169068, 12135053, 12169013, 12170010, 12138013, 12156019, 12154016, 12132051, 12134008, 12126088, 12156057,

12162032, 12138010, 12169041, 12156014, 12170033, 12160007, 12168058, 12162043, 12158073, 12137008, 12137007, 12156062, 12156058, 12136069, 12136065, 12167008, 12158067, 12169033, 12169032, 12134006, 12164045, 12133053, 12127009, 12155049, 12168057, 12168054, 12149049, 12169044, 12158053, 12155005, 12161013, 12161011, 12170029, 12136046, 12133060, 12162017, 12162030, 12150036, 12157022, 12170009, 12138011, 12150039, 12134059, 12157045, 12135054, 12161007, 12161056, 12161033, 12161031, 12153017, 12152010, 12169054, 12160018, 12157011, 12150048, 12157014, 12150057, 12157023, 12153015, 12157017, 12132044, 12138024, 12137005, 12167041, 12149039, 12126092, 12151065, 12134045, 12159003, 12159004, 12167046, 12135007, 12167010, 12161005, 12138023, 12128031, 12164064, 12162016, 12127022, 12155017, 12136005, 12155011, 12157040, 12169018, 12169061, 12155014, 12134046, 12149036, 12155044, 12138021, 12155006, 12159036, 12158061, 12168001, 12133008, 12150002, 12158027, 12149038, 12132022, 12161027, 12165024, 12132014, 12132010, 12136075, 12165038, 12170057, 12128024, 12128015, 12171007, 12128018, 12155059, 12155063, 12169066, 12128025, 12162005, 12128030, 12161015, 12169063, 12169048, 12156065, 12157025, 12167048, 12167047, 12127035, 12171016, 12162009, 12161010, 12154048, 12160002, 12133025, 12133040, 12154046, 12132047, 12161055, 12154018, 12164046, 12168062, 12151056, 12153021, 12159013, 12159025, 12127021, 12153016, 12134052, 12133054, 12160003, 12134047, 12151040, 12162012, 12155002, 12168004, 12154013, 12162033, 12136026, 12135045, 12135050, 12157047, 12149061, 12132071, 12158006, 12155023, 12127046, 12132065, 12161020, 12132018, 12132025, 12161016, 12162034, 12160001, 12170017, 12162044, 12137022, 12158052, 12132011, 12132009, 12163052, 12151069, 12151044, 12134061, 12133004, 12158017, 12132049, 12155021, 12132050, 1216501612165010, 12165009, 12137010, 12135041, 12135025, 12135038, 12135021, 12135039, 12135027, 12135042, 12135029, 12135023, 12135019, 12136076, 12152005, 12136006, 12136055, 12135012, 12155039, 12134011, 12155030, 12171015, 12134010, 12134036, 12134034, 12134037, 12134038, 12134040, 12154006, 12154005, 12154017, 12154012, 12128038, 12146007, 12149037, 12163053, 12171004, 12161028, 12153013, 12163022, 12170015, 12156023, 12156034, 12168002, 12137020, 12162035, 12135031, 12133058, 12135028, 12162004, 12165029, 12133059, 12154007, 12154009, 12151038, 12128017, 12137014, 12151016, 12160024, 12128016, 12135020, 12169015, 12149034, 12170025, 12151039, 12136086, 12136085, 12159040, 12158060, 12161061, 12170001, 12134057, 12135011, 12152013, 12158001, 12158002, 12150047, 12153033, 12163016, 12132017, 12132019, 12128028, 12135048, 12162046, 12163014, 12157041, 12158015, 12133024, 12151046, 12134017, 12162028, 12132063, 12132056, 12132058, 12132072, 12132064, 12133013, 12133016, 12133012, 12133005, 12133010, 12160020, 12133061, 12134001, 12162015, 12136039, 12154002, 12132057, 12168061, 12135052, 12158040, 12169034, 12163005, 12156031, 12132013, 12155036, 12169031, 12134068, 12151041, 12134018, 12168064, 12165013, 12164011, 12169026, 12134009, 12156059, 12169029, 12170035, 12164084, 12164051, 12132069, 12165002, 12135056, 12128021, 12170016, 12158070, 12162006, 12156066, 12166060, 12127050, 12156036, 12137027, 12134049, 12165025, 12165031, 12155066, 12161053, 12134051, 12151003, 12170043, 12136048, 12138008, 12128008, 12128009, 12137038, 12137042, 12152007, 12137041, 12132052, 12132055, 12152014, 12151068, 12136084, 12134014, 12138017, 12134050, 12158058, 12158074, 12158068, 12156063, 12161029, 12164089, 12132046, 12154021, 12161060, 12137030, 12150014, 12169025, 12166011, 12136081, 12170006, 12135026, 12161058, 12136052, 12150016, 12133020, 12136082, 12154068, 12168063, 12163058, 12135059, 12133021, 12132008, 12127042, 12170030, 12127041, 12152006, 12152009, 12128012, 12135003, 12128032, 12154014, 12150027, 12160017, 12132023, 12132020, 12163015, 12134066, 12132032, 12132033, 12154039, 12151032, 12128014, 12135061, 12162021, 12162020, 12164065, 12135044, 12134053, 12134063, 12132054, 12170007, 12133014, 12137036, 12162008, 12136002, 12164063, 12134023, 12132048, 12137011, 12170034, 12158069, 12127019, 12155022, 12155056, 12137015, 12132026, 12127030, 12127020, 12168056, 12134003, 12134003

Run numbers, for pp 200 GeV Run9 data, are analyzed

10110061, 10110062, 10110064, 10110065, 10110073, 10110074, 10111005, 10111021, 10111043, 10111044, 10111045, 10111046, 10111047, 10111048, 10111050, 10111051, 10111055, 10111056, 10111058, 10111059, 10111061, 10111064, 10111170, 10111181, 10112018, 10112019, 10112021, 10112024, 10112025, 10112026, 10112029, 10112038, 10112039, 10112040, 10112041, 10112043, 10112044, 10112045, 10112048, 10112099, 10112105, 10112108, 10112109, 10112111, 10112112, 10113010, 10113011, 10113012, 10113015, 10113021, 10113022, 10113023, 10113066, 10113068, 10113073, 10113074, 10113075, 10113084, 10113085, 10113086, 10113088, 10113089, 10113090, 10113104, 10114016, 10114021, 10114024, 10114025, 10114026, 10114027, 10114028, 10114029, 10114030, 10114031, 10114032, 10114033, 10114034, 10114037, 10114038, 10114053, 10114054, 10114070, 10114071, 10114074, 10114077, 10114078, 10114079, 10114080, 10114081, 10114082, 10114084, 10114087, 10114088, 10114089, 10114090, 10115017, 10115019, 10115020, 10115021, 10115025, 10115026, 10115027, 10115028, 10115029, 10115031, 10115032, 10115033, 10115034, 10115037, 10115038, 10115039, 10115040, 10115041, 10115042, 10115043, 10115050, 10115051, 10115052, 10115053, 10115066, 10115067, 10115072, 10115073, 10115074, 10115077, 10115082, 10115083, 10115086, 10115089, 10115094, 10115096, 10116003, 10116009, 10116010, 10116011, 10116012, 10116015, 10116016, 10116018, 10116019, 10116030, 10116031, 10116032, 10116033, 10116042, 10116047, 10116048, 10116051, 10116052, 10116053, 10116054, 10116055, 10116056, 10117003, 10117004, 10117012, 10117013, 10117014, 10117017, 10117027, 10117028, 10117039, 10117040, 10117041, 10117042, 10117043, 10117044, 10117045, 10117046, 10117051, 10117052, 10117085, 10117086, 10117087, 10118003, 10118007, 10118008, 10118011, 10118012, 10118015, 10118018, 10118021, 10118022, 10120014, 10120015, 10120019, 10120020, 10120021, 10120023, 10120024, 10120025, 10120063, 10120065, 10120078, 10120079, 10120082, 10120085, 10120086, 10120093, 10120097, 10120100, 10121001, 10121017, 10121020, 10121022, 10121029, 10121039, 10121040, 10121043, 10121044, 10121088, 10121091, 10121092, 10121093, 10121094, 10121095, 10121096, 10121097, 10122006, 10122007, 10122010, 10122013, 10122014, 10122015, 10122016, 10122017, 10122019, 10122022, 10122023, 10122024, 10122047, 10122048, 10122049, 10122050, 10122053, 10122054, 10122055, 10122060, 10122061, 10122065, 10122067, 10122071, 10122086, 10122087, 10122095, 10122098, 10122099, 10123004, 10123007, 10123010, 10123013, 10123014, 10123015, 10123086, 10123087, 10123088, 10123090, 10124011, 10124012, 10124013, 10124014, 10124037, 10124038, 10124044, 10124045, 10124046, 10124049, 10124050, 10124053, 10124055, 10124057, 10124062, 10124066, 10124071, 10124072, 10124075, 10124076, 10124110, 10124111, 10124113, 10125001, 10125008, 10125009, 10125010, 10125014, 10125015, 10125016, 10125017, 10125022, 10125023, 10149086, 10151061, 10159008, 10159020, 10159022, 10159023, 10159024, 10159043, 10159047, 10165072, 10165074, 10166051, 10166054, 10166060, 10166064, 10166065, 10179001, 10180002, 10180034, 10125055, 10125065, 10125066, 10125068, 10125069, 10125075, 10125076, 10125080, 10125083, 10125091, 10126003, 10126004, 10126005, 10126012, 10126016, 10126017, 10126018, 10126019, 10126024, 10126025, 10126026, 10126040, 10126041, 10126046, 10126047, 10126052, 10126064, 10126067, 10126068, 10126069, 10126073, 10126074, 10126075, 10126080, 10126081, 10126082, 10126083, 10126084, 10126087, 10126088, 10126089, 10126090, 10127007, 10127008, 10127009, 10127010, 10127011, 10127047, 10128001, 10128002, 10128003, 10128004, 10128008, 10128010, 10128012, 10128019, 10128020, 10128021, 10128026, 10128027, 10128029, 10128030, 10128031, 10128032, 10128036, 10128041, 10128043, 10128046, 10128047, 10128048, 10128049, 10128050, 10128052, 10128053, 10128054, 10128055, 10128056, 10128059, 10128060, 10128061, 10128063, 10128065, 10128066, 10128070, 10128071, 10128072, 10128094, 10128098, 10128099, 10128100, 10128101, 10128102, 10129003, 10129005, 10129006, 10129007, 10129008, 10129011, 10129029, 10129030, 10129032, 10129047, 10129048, 10129049, 10129050, 10130011, 10130012, 10130014, 10130015, 10131009, 10131011, 10131012, 10131029, 10131030, 10131031, 10131034, 10131039, 10131040, 10131041, 10131042, 10131043, 10131044, 10131045, 10131047, 10131052, 10131075, 10131076, 10131083, 10131087, 10131088, 10131090,

10131091, 10131092, 10131094, 10132001, 10132003, 10132004, 10132008, 10132009, 10132010, 10132011, 10132012,
10134017, 10134021, 10134024, 10134025, 10134026, 10134027, 10134028, 10134030, 10134035, 10134036, 10134037,
10134044, 10134085, 10134086, 10134101, 10134102, 10134103, 10135001, 10135002, 10135005, 10135006, 10135007,
10135008, 10135009, 10135011, 10135016, 10135017, 10135018, 10135030, 10135058, 10135059, 10135063, 10135064,
10135065, 10135066, 10135070, 10135072, 10135076, 10135077, 10135081, 10135082, 10135083, 10136001, 10136010,
10136011, 10136012, 10136017, 10136019, 10136020, 10136021, 10136024, 10136025, 10136026, 10136027, 10136028,
10136029, 10136030, 10136031, 10136035, 10136036, 10136037, 10136041, 10136042, 10136061, 10136063, 10136069,
10136070, 10136071, 10136073, 10136074, 10136077, 10136078, 10136079, 10136080, 10136092, 10136096, 10136097,
10136099, 10136100, 10137003, 10137004, 10137006, 10137008, 10137045, 10137046, 10137047, 10137048, 10137049,
10137051, 10137052, 10137055, 10137059, 10137060, 10137061, 10137063, 10137064, 10137065, 10137066, 10137067,
10138008, 10138011, 10138012, 10138013, 10138014, 10138016, 10138021, 10138022, 10138023, 10138024, 10138025,
10138026, 10138027, 10138030, 10138032, 10138047, 10138048, 10138049, 10138052, 10138053, 10138054, 10138055,
10138081, 10138083, 10138087, 10138088, 10138091, 10138095, 10138098, 10138099, 10138100, 10139001, 10139002,
10139003, 10139007, 10139008, 10139009, 10139010, 10139014, 10139015, 10139017, 10139018, 10139031, 10139038,
10139040, 10139043, 10139044, 10139067, 10139068, 10139069, 10139070, 10139073, 10139074, 10139076, 10139077,
10139078, 10139102, 10139107, 10140002, 10140005, 10140006, 10140007, 10140010, 10140011, 10141008, 10141010,
10141011, 10141013, 10141015, 10141018, 10141019, 10141020, 10141023, 10141025, 10141026, 10141027, 10141030
, 10141031, 10141032, 10142011, 10142012, 10142019, 10142020, 10142023, 10142029, 10142031, 10142032, 10142034,
10142035, 10142036, 10142041, 10142042, 10142043, 10142044, 10142045, 10142046, 10142047, 10142050, 10142056,
10142057, 10142058, 10142085, 10142086, 10142092, 10142093, 10142098, 10143007, 10143008, 10143009, 10143014,
10143015, 10143018, 10143023, 10143025, 10143026, 10143027, 10143029, 10143043, 10143044, 10143045, 10143046,
10143047, 10143051, 10143052, 10143053, 10143054, 10143055, 10143058, 10143060, 10143061, 10143062, 10143063,
10143064, 10143065, 10143076, 10143077, 10143078, 10143082, 10143083, 10143085, 10143086, 10143090, 10143091,
10143092, 10143095, 10143098, 10143099, 10143102, 10143103, 10143104, 10143106, 10144001, 10144002, 10144003,
10144022, 10144026, 10144027, 10144028, 10144029, 10144030, 10144033, 10144034, 10144035, 10144036, 10144037,
10144038, 10144044, 10144045, 10144046, 10144047, 10144066, 10144067, 10144072, 10144073, 10144074, 10144075,
10144076, 10144082, 10144083, 10144084, 10144085, 10144086, 10144087, 10144090, 10144091, 10144092, 10144093,
10144097, 10144098, 10144099, 10145011, 10145012, 10145013, 10145016, 10145018, 10145027, 10145030, 10145032,
10145034, 10145036, 10145038, 10145042, 10145046, 10145047, 10145070, 10145071, 10145072, 10145073, 10145076,
10145078, 10145079, 10145081, 10145082, 10145083, 10146040, 10146041, 10146043, 10146046, 10146047, 10146048,
10146049, 10146050, 10146051, 10146052, 10146054, 10146055, 10146073, 10146084, 10146086, 10146087, 10146091,
10147124, 10148002, 10148005, 10148006, 10148021, 10148025, 10148026, 10148027, 10148028, 10148033, 10148034,
10148035, 10148036, 10149001, 10149008, 10149012, 10149023, 10149024, 10149025, 10149026, 10149028, 10149031,
10149032, 10149033, 10149034, 10149035, 10149036, 10149078, 10149087, 10150001, 10150005, 10150008, 10150009,
10150010, 10150011, 10150012, 10150013, 10150018, 10150021, 10150022, 10150023, 10150024, 10150025, 10150051,
10150052, 10150053, 10150056, 10150057, 10151001, 10151002, 10151003, 10151004, 10151005, 10151006, 10151015,
10151034, 10151035, 10151039, 10151040, 10151041, 10151042, 10151043, 10151044, 10151045, 10151046, 10151047,
10151050, 10151057, 10151060, 10152001, 10152004, 10152005, 10152006, 10152007, 10152008, 10152009, 10152010,
10154060, 10154061, 10154064, 10154065, 10154066, 10154067, 10154068, 10154069, 10154083, 10155001, 10155010,
10155011, 10155014, 10155015, 10155016, 10155018, 10155019, 10155020, 10155022, 10155095, 10155097, 10156004,
10156007, 10156008, 10156009, 10156011, 10156013, 10156022, 10156031, 10156034, 10156037, 10156038, 10156039,
10156040, 10156058, 10156086, 10156087, 10156090, 10156091, 10156092, 10156093, 10156095, 10156096, 10157001,
10157004, 10157005, 10157015, 10157016, 10157019, 10157020, 10157021, 10157022, 10157023, 10157027, 10157051,
10157052, 10157053, 10157056, 10157057, 10157058, 10157059, 10157060, 10158001, 10158004, 10158010, 10158013,
10158014, 10158015, 10158016, 10158017, 10158018, 10158021, 10158042, 10158043, 10158046, 10158047, 10158048,
10158049, 10158050, 10158051, 10158054, 10158055, 10158074, 10158075, 10158076, 10158079, 10158080, 10158082,
10158083, 10158086, 10158087, 10158089, 10158090, 10159006, 10159039, 10159040, 10159044, 10159045, 10159046,
10159048, 10159049, 10160005, 10160006, 10160009, 10160010, 10160011, 10160012, 10160013, 10160014, 10160015,
10160016, 10160017, 10160024, 10160067, 10160068, 10160069, 10160070, 10160071, 10160072, 10160075, 10160076,
10160077, 10160078, 10160079, 10160081, 10160084, 10161005, 10161006, 10161010, 10161011, 10161014, 10161015,
10161016, 10161019, 10161020, 10161021, 10161022, 10161023, 10161024, 10161025, 10161026, 10161027, 10161030,
10162006, 10162007, 10162010, 10162024, 10162025, 10162028, 10162029, 10162030, 10162031, 10162032, 10162033,
10162034, 10162035, 10162036, 10162037, 10162038, 10162040, 10163007, 10163008, 10163009, 10163010, 10163011,
10163048, 10163051, 10163052, 10163053, 10163054, 10163055, 10163056, 10163059, 10164002, 10164009, 10164010,
10164011, 10164013, 10164016, 10164017, 10164018, 10164025, 10164026, 10164029, 10164030, 10164031, 10164034,
10164057, 10164060, 10164061, 10164062, 10164067, 10164078, 10164079, 10164082, 10165007, 10165008, 10165011,
10165013, 10165014, 10165015, 10165016, 10165017, 10165018, 10165019, 10165020, 10165022, 10165023, 10165024,
10165027, 10165041, 10165042, 10165043, 10165046, 10165047, 10165048, 10165049, 10165050, 10165051, 10165052,
10165053, 10165054, 10165057, 10165070, 10165077, 10165078, 10165079, 10165080, 10165081, 10166001, 10166003,
10166012, 10166021, 10166022, 10166023, 10166024, 10166025, 10166026, 10166027, 10166028, 10166061, 10166063,
10166067, 10167007, 10167008, 10167009, 10167012, 10167013, 10167014, 10167015, 10167016, 10167017, 10167020,
10167048, 10167049, 10167050, 10167053, 10167054, 10167056, 10167057, 10167058, 10167059, 10167067, 10167068,
10167069, 10169005, 10169006, 10169009, 10169010, 10169011, 10169012, 10169013, 10169014, 10169015, 10169020,
10169021, 10169030, 10169031, 10169032, 10169033, 10169041, 10169042, 10169043, 10169044, 10169047, 10169048,
10169049, 10169050, 10169065, 10169070, 10169074, 10169075, 10169076, 10169077, 10169078, 10169079, 10169080,
10170003, 10170011, 10170012, 10170013, 10170016, 10170017, 10170018, 10170019, 10170020, 10170023, 10170024,
10170025, 10170026, 10170029, 10170045, 10170046, 10170047, 10170050, 10170051, 10170052, 10170053, 10170054,
10170060, 10170061, 10170064, 10170065, 10170075, 10170078, 10170080, 10170081, 10170089, 10171008, 10171009,
10171011, 10171014, 10171015, 10171016, 10171019, 10171021, 10171022, 10171025, 10171026, 10171034, 10171036,
10171037, 10171041, 10171042, 10171043, 10171044, 10171045, 10171048, 10171060, 10171061, 10171068, 10171069,
10171070, 10171071, 10171078, 10172001, 10172002, 10172003, 10172007, 10172016, 10172017, 10172018, 10172021,
10172022, 10172023, 10172024, 10172025, 10172026, 10172028, 10172054, 10172055, 10172056, 10172057, 10172058,
10172059, 10172060, 10172061, 10172064, 10172077, 10172078, 10172079, 10172082, 10172083, 10172085, 10172089,
10172090, 10172091, 10172094, 10173007, 10173008, 10173009, 10173012, 10173013, 10173014, 10173015, 10173016,
10173017, 10173031, 10173032, 10173033, 10173039, 10173046, 10173048, 10173051, 10173052, 10173053, 10173054,
10173055, 10173077, 10173078, 10173081, 10173082, 10173083, 10173084, 10173085, 10173087, 10173088, 10173090,
10174001, 10174012, 10174013, 10174016, 10174017, 10174021, 10174022, 10174023, 10174024, 10174025, 10174026,
10174027, 10174028, 10174031, 10174044, 10174045, 10174048, 10174049, 10174050, 10174051, 10174052, 10174068,

10174071, 10174072, 10174073, 10174076, 10174078, 10174079, 10174080, 10174083, 10174093, 10174094, 10175001, 10175004, 10175005, 10175008, 10175009, 10175010, 10175011, 10175012, 10175013, 10175014, 10175019, 10175038, 10176001, 10176008, 10176016, 10176017, 10176018, 10176020, 10176022, 10176025, 10176028, 10177007, 10177008, 10177009, 10177014, 10177016, 10177017, 10177018, 10177019, 10177022, 10177024, 10177055, 10177056, 10177057, 10177060, 10177061, 10178022, 10178023, 10178026, 10178029, 10178036, 10178037, 10179002, 10179005, 10179006, 10179007, 10179008, 10179009, 10179010, 10179018, 10179019, 10179022, 10179031, 10179032, 10179033, 10179036, 10179042, 10179043, 10179044, 10179045, 10179059, 10179060, 10179061, 10179064, 10179065, 10179072, 10179073, 10179074, 10179077, 10179085, 10179086, 10179088, 10179096, 10179097, 10179098, 10180003, 10180004, 10180007, 10180020, 10180021, 10180022, 10180027, 10180028, 10180029, 10180030, 10181005, 10135055, 10135069, 10142037, 10142037

0.3 Efficiency of charge hadrons

The efficiency of charge hadrons are estimated from Run-11 embedding samples for AuAu 200 GeV.

/eliza17/star/starprod/embedding/AuAu200_production_2011/

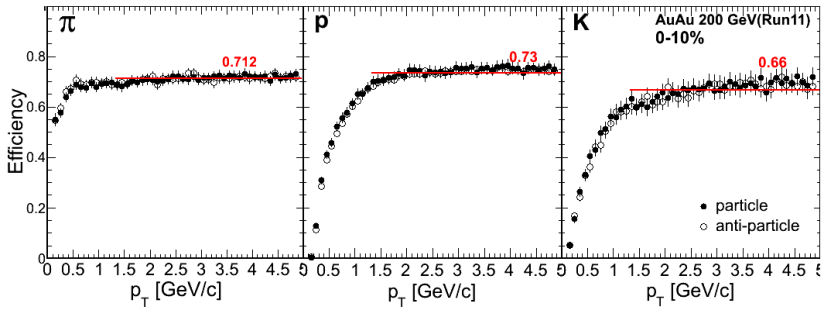

Figure 6: TPC tracking Efficiency vs transverse momentum for different particles species for AuAu 200 GeV Run-11 at 0-10% centrality.

Here, These efficiencies are estimated from the embedding sample using same track and vertex cut as the data analysis. For the estimation of efficiency, it is assume that total charge particles are collection of protons, pions, and kaons, and their anti-particles. Expression for positive charged particle efficiency,

$$\varepsilon_{+} = w_p \varepsilon_P + w_{K^+} \varepsilon_{K^+} + w_{\pi^+} \varepsilon_{\pi^+}, \tag{1}$$

Here $w_p + w_{K^+} + w_{\pi^+} = 1$. Where w_x and ε_x are the percentage and efficiency of particles species x. w_x is estimated from the particle ratio for different charged particles like, $\frac{p}{\pi^+}$, $\frac{\bar{p}}{\pi^-}$, $\frac{K^+}{\pi^+}$, $\frac{K^-}{\pi^-}$, and ε_x is estimated by integrated p_T dependance efficiency using expression

$$\varepsilon_{+} = \frac{\int \varepsilon_{+}(p_T) f(p_T) p_T dp_T}{\int f(p_T) p_T dp_T}. \tag{2}$$

Here p_T < 1.2 GeV/c is used.

Fig.7 represents tracking efficiency for pions and anti-pions as a function of refmult.

It is found that efficiency of total charged hadrons for AuAu 200 GeV is 71.2% for $0-10\%$ centrality. Fig 6, is the efficiency vs transverse momentum plot for different particles species for AuAu 200 GeV Run-11 at 0-10% centrality

Where as, in case of pp, efficiency 91% is used.

0.4 Correlation functions

The $\Delta\phi$ correlation functions for π^0_{rich} and γ_{rich} trigger with charged hadrons for AuAu collisions at 0-10% centrality (Fig. 8) and that for pp (Fig. 9) are shown. After using TSP cuts, as discussed in Section 0.8, $\Delta\phi$ correlation are made for both π^0_{rich} and γ_{rich} with all charged hadrons using BEMC cluster information (for TSP) and TPC tracks. In case of AuAu collisions, after subtracting flow modulated backgrounds, as discussed in Section-0.5, the away-side (AS) and near-side (NS) yields are extracted and then corrected for efficiency (Section-0.3). For the extraction of AS and NS yields, both for π^0_{rich} and γ_{rich} trigger, $|\Delta\phi| < 1.3$ and $|\Delta\phi - \pi| < 1.3$ are used, respectively. In case of pp, same $\Delta\phi$ window and same TSP cuts are used. Due to significantly low backgrounds in pp w.r.t AuAu collisions, by selecting suitable ZYAM windows (same for AuAu for normalizing mixed event/flat background) backgrounds are subtracted for AS and NS yields. This method is discussed in one of our PWG presentation [7]. The systematic effects of varying yield extraction windows and ZYAM windows are checked and the systematic uncertainty due to these, are considered.

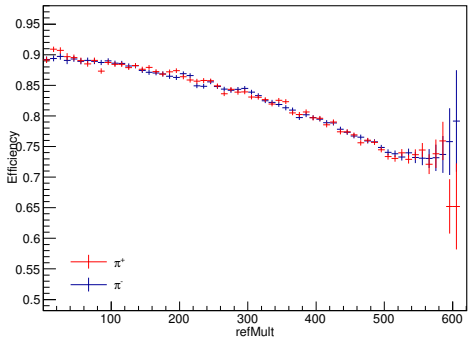

Figure 7: TPC tracking Efficiency, for pions and anti-pions, vs refmult for AuAu 200 GeV Run11.

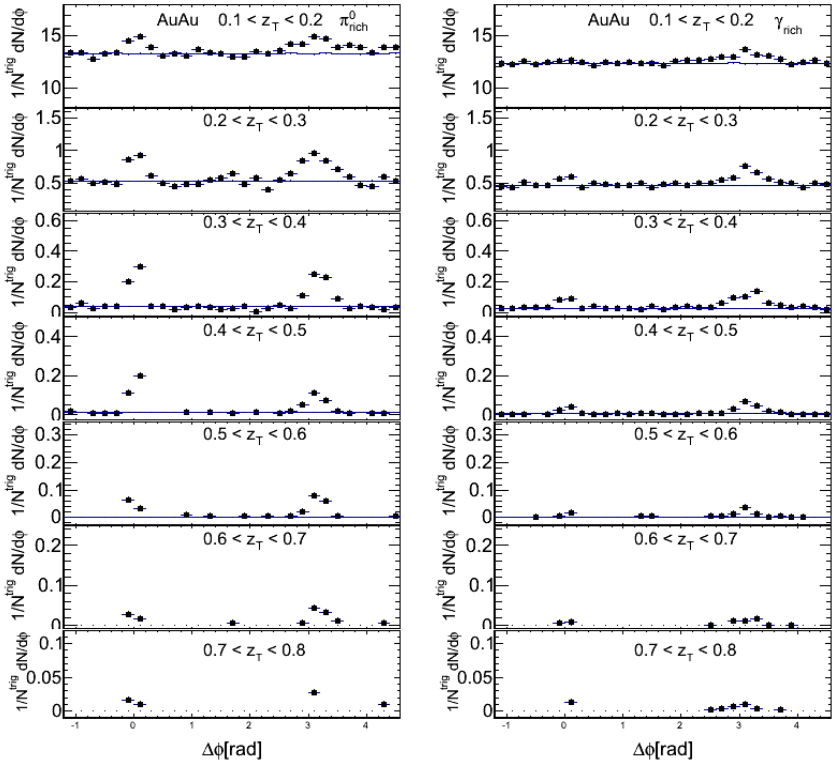

Figure 8: $\Delta\phi$ correlation functions of π^0_{rich} and γ_{rich} trigger with charged hadrons for AuAu collisions at 0-10% centrality. Each panels represent different z_T bins, where filled markers represent correlation functions from data and line represents flow modulated normalized backgrounds.

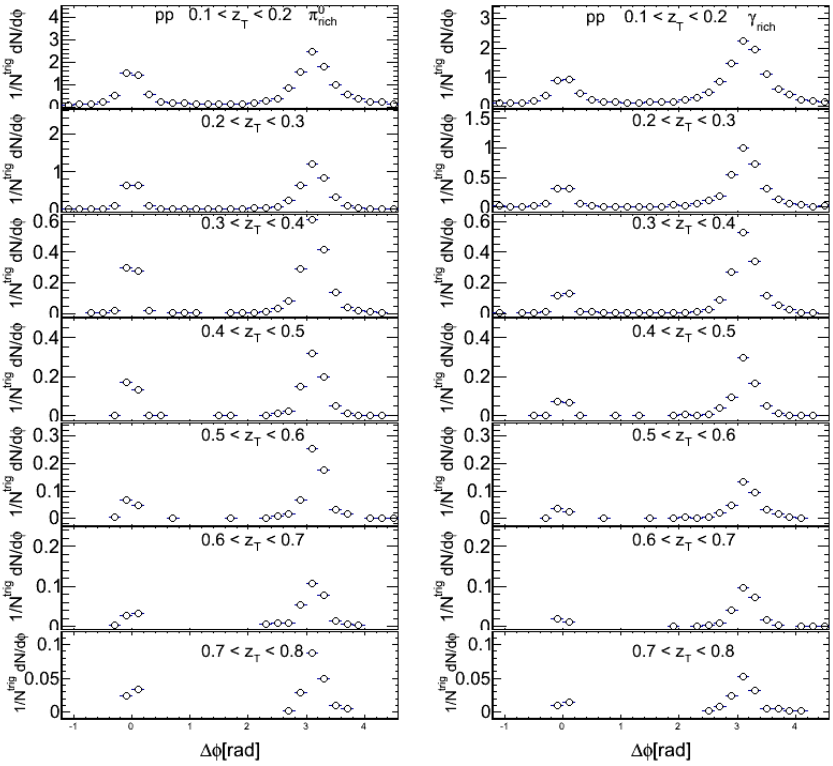

Figure 9: $\Delta\phi$ correlation functions of π^0_{rich} and γ_{rich} trigger with charged hadrons for pp collisions. Each panels represent different z_T bins, where filled markers represent correlation functions from data.

0.5 Background subtraction

Background subtraction from $\Delta\phi$ correlation functions for different z_T, between trigger γ^{dir} and π^0 with charged hadrons, are based on modulated background due to elliptic flow using following formula,

$$B[1 + 2 < v_2^{trig} >< v_2^{assoc} > cos(2\Delta\phi)] \tag{3}$$

Here B is the constant that is determined from the normalized mixed events. The detail discussion of the mixed event technique has been discussed in Section-0.6. $< v_2^{trig} >$ and $< v_2^{assoc} >$ are the average v_2 for trigger particles and associated charged hadrons, respectively. The determination of v_2 component has been discussed in section 0.7. These flow contributions are dominant mainly at low z_T bins, up-to 0.1 to 0.3, because of contribution of low momentum particles are these z_T bins.

The value of B are determined by selecting ZYAM windows. In this analysis both for AuAu and pp, ZYAM window [0.99,1.31] is used as default. Different systematic checks have been done by varying ZYAM windows for this analysis. After subtracting these flow modulated background from $\Delta\phi$ correlation functions both for trigger γ^{dir} and π^0 for each z_T bins, the yields of the associated charged hadrons are extracted. In the next section, the mixed events for background subtraction method have been discussed.

At high z_T bins, backgrounds counts are zero for $\Delta\phi$ correlation functions for both trigger γ_{rich} and π^0_{rich} at $0.5 < z_T$. Hence for correlation functions having zero background, at higher z_T bins, error of that background are determined from that extrapolated background assuming 100% error ($N \pm \sqrt{N}$) of that z_T bins. The error of extrapolated background is determined from the Fig 10. The exponential fit functions are used.

0.6 Mixed events for background subtraction

In the mixed events technique, we try to keep all event characteristics same as possible as our data analysis. The event mixing are done for a unit Refmult and $|\Delta V_Z|$ = 5 cm from -55< V_Z <55 cm. All tracks and towers informations same as our analysis condition. Here the randomly chosen trigger tower are correlated with randomly selected associated particles from different events. The schematic representation below shows how it has been done. In order to introduce event-by-event (e-b-e) fluctuations in event mixing, the no. of associated tracks per event are selected based on the Poisson distribution with mean equal to mean of the real data distribution. Figure 12 shows average associate mult. vs refmult and mult. vs refmult. The correlation functions for data and mixed events, in different z_T bins, are shown in Fig 13. It is observed that the background fluctuations are well explained by the acceptance corrected mixed events. But some z_T bins, it is observed also that the background fluctuations, may be from statistical in nature, are not reproduced by the mixed events. In order to minimize the effect of this statistical fluctuations, the stat. error of the background are taken into account while subtracting background, from $\Delta\phi$ correlation function after normalizing background.

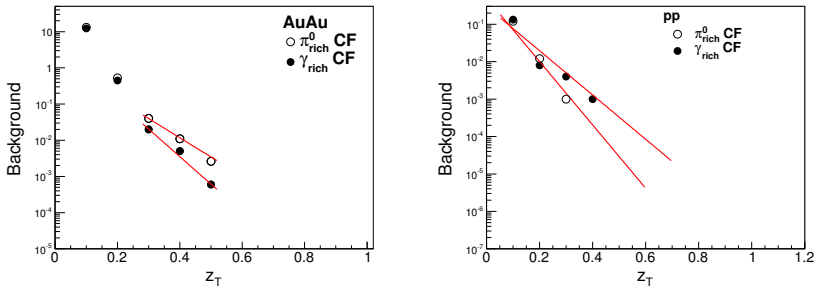

Figure 10: Backgrounds are extrapolated for higher z_T bins for AuAu (left panel) and pp (right panel) collisions. In case of AuAu, the exponential function obtained from fit function are, for π^0_{rich} and γ_{rich}, $B_{extrapolated} = 1.55 * 1/Exp(12.22 * z_T)$ and $B_{extrapolated} = 8.0 * 1/Exp(19.5 * z_T)$ respectively. Similarly, in pp the exponential function obtained from fit function are, for π^0_{rich} and γ_{rich}, $B_{extrapolated} = 0.3 * 1/Exp(13.62 * z_T))$ and $B_{extrapolated} = 0.5 * 1/Exp(19.5 * z_T)$ respectively.

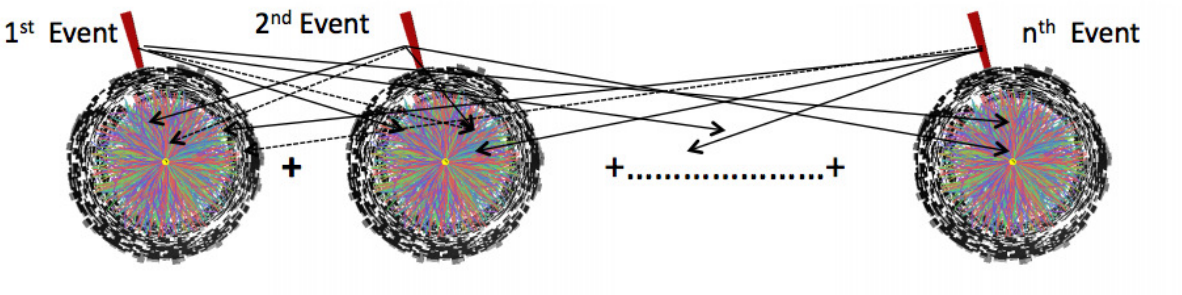

Figure 11: The schematic represtation of mixed events.

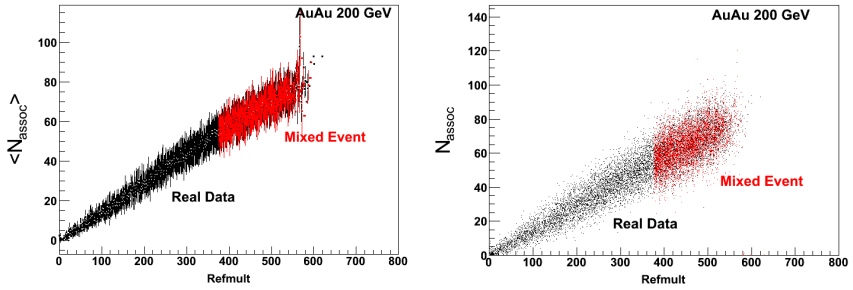

Figure 12: Average associate mult. vs refmult and mult. vs refmult to show e-b-e fluctuation in mixed events describe the data well.

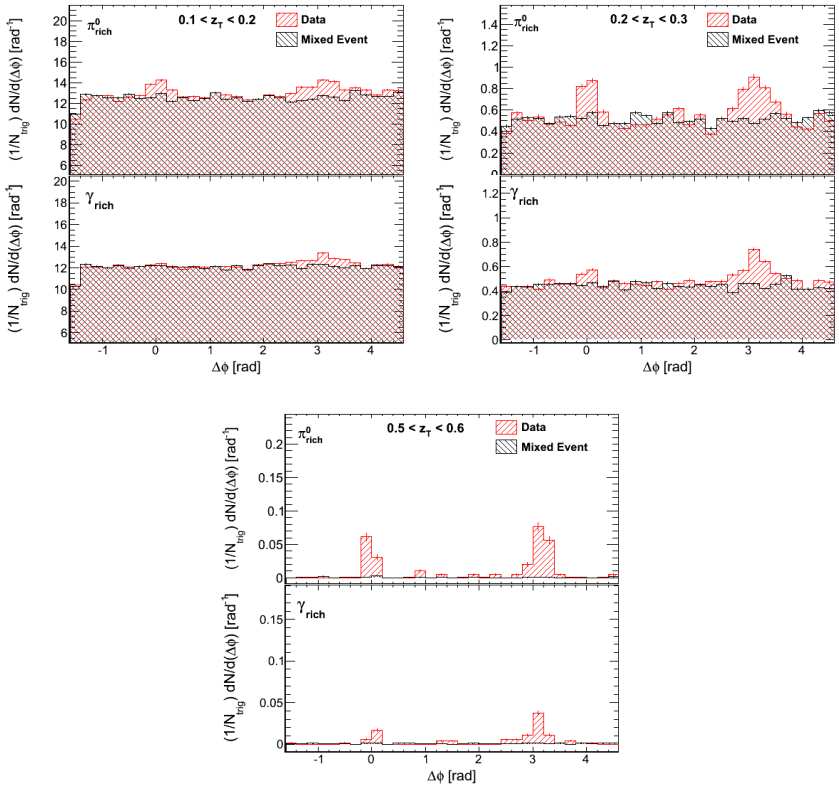

Figure 13: Correlation functions from data and mixed events for three z_T bins for AuAu collisions at 0-10% centrality.

0.7 Determination of flow (v_2) component

In order to subtract, flow component from $\Delta\phi$ correlation function between trigger γ^{dir} and π^0 with charged hadrons, at low p_T^{assoc} ($1.2 < p_T^{assoc}$ GeV/c), we used parameterized v_2 for charged particles. Detail study about flow parameterization can be found in this link

(http://www.star.bnl.gov/protected/jetcorr/mvl/v2_compare/auau_compare.html).

Here is the plots for v_2 vs. p_T for AuAu 200 GeV (0-10%) based on STAR published results and its flow parameterization function. The results for $< v_2 >$ vs. z_T is shown below. To calculate $< v_2 >$ for different z_T bins, we use this formula, $< v_2 >= \frac{\int v_2(p_T) f(p_T) p_T dp_T}{\int f(p_T) p_T dp_T}$.

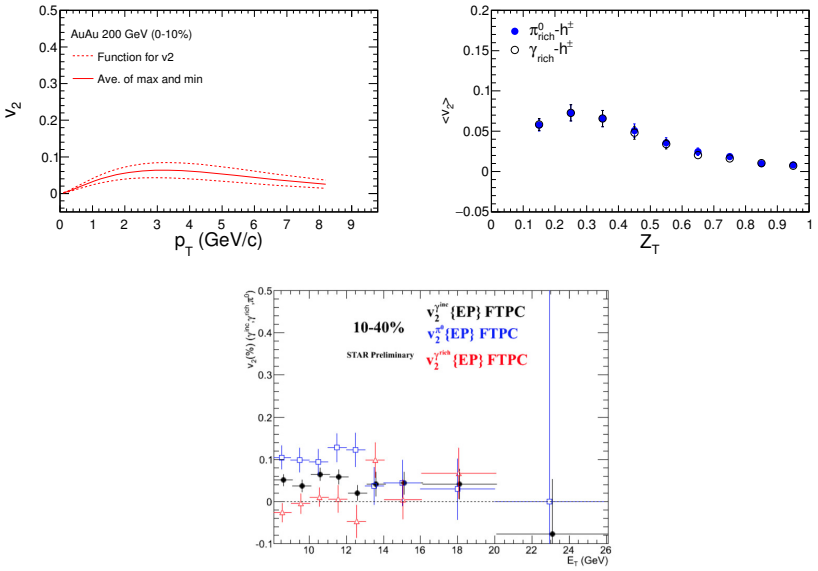

Figure 14: Upper panels for parametrized form of v_2 and $< v_2 >$ and lower panel for v_2 for γ^{rich} and π^0_{rich}.

In order to subtract flow (mainly v_2) contribution along with background, from azimuthal correlation functions, following formula is used,

$$B[1 + 2 < v_2^{trig} >< v_2^{assoc} > cos(2\Delta\phi)]$$

Here $< v_2^{trig} >$ is the trigger v_2 value. here v_2 values of γ^{rich} and π^0_{rich} are used for background subtraction. Whereas $< v_2^{assoc} >$ is taken from above plot for given z_T. The $< v_2 >$ values are taken 0.001 and 0.13 ± 0.05 for γ^{rich} and π^0_{rich} respectively.

0.8 Transverse Shower Profile

In this analysis, events having at least one BSMD cluster (one/two towers depending on relative position of the cluster to the tower's center) with energy E_T >8 GeV are selected. A trigger tower is rejected if it has a track with p > 3.0 GeV/c pointing to it. In order to, discriminate between γ and π^0 depends on an analysis of the shower shape, as measured by the BSMD and BEMC [2]. In Transverse Shower Profile (TSP) technique, TSP is defined as

$$TSP = \frac{E_{cluster}}{\sum_i e_i r_i^{1.5}} \tag{4}$$

Here, $E_{cluster}$ is cluster energy, e_i is the BSMD strip energy and r_i is the distance of the strip from the center of the cluster. Exponent in r_i is decided based on the best discrimination results obtained between π^0/γ sample from simulation study.

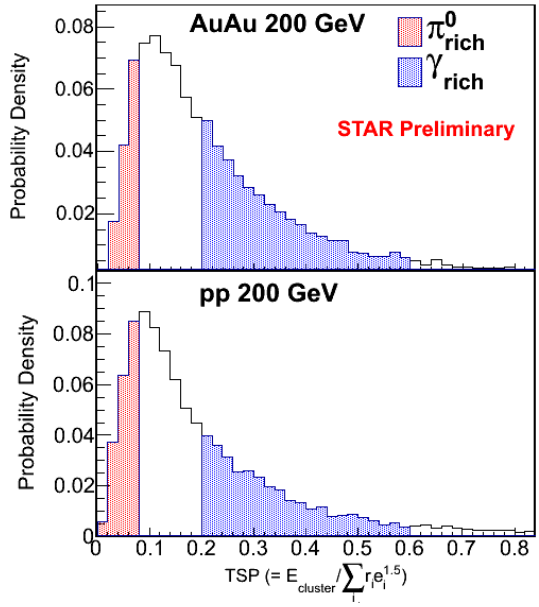

Figure 15: TSP probability distribution for AuAu and pp.

TSP cuts are tuned to get

- a nearly pure sample of π^0 (called "π^0_{rich}"): TSP < 0.08
- a sample with enhanced fraction of γ^{dir}(called "γ_{rich}"): 0.2<TSP<0.6

0.8.1 Extraction of associated Yields of γ^{dir} and π^0 trigger

Near-side and away-side charged hadrons yields are extracted within $|\Delta\phi| \leq 1.3$ and $|\Delta\phi - \pi| \leq 1.3$ both for π^0_{rich} and γ_{rich} trigger. Extracted raw yields are corrected for charge particle reconstruction efficiency. Extraction of γ^{dir} associated yields, for different z_T bins, are done, by assuming near side γ^{dir} associated hadron yield is zero. The γ^{dir} associated away-side yields is given by,

$$Y_{\gamma_{dir}+h} = \frac{Y^a_{\gamma_{rich}+h} - RY^a_{\pi^0+h}}{1-R} \tag{5}$$

Where,

$$R = \frac{Y^n_{\gamma_{rich}+h}}{Y^n_{\pi^0+h}} \tag{6}$$

$$1 - R = \frac{N^{\gamma^{dir}}}{N^{\gamma_{rich}}} \tag{7}$$

Here, $Y^{a(n)}_{\gamma_{rich}+h}$ and $Y^{a(n)}_{\pi^0+h}$ are away-side (near-side) yields of associated particles per γ_{rich} and π^0 trigger, respectively. The stat. error for the $Y_{\gamma_{dir}+h}$ are calculated by using error propagation method, details can be found in section 0.9.

The values of $(1-R)$ are found to be $\sim 40\%$ and $\sim 70\%$ for pp and AuAu central $(0-10\%)$ collisions, respectively. In the fig 28, the values of R for different z_T are plotted for AuAu and pp collisions.

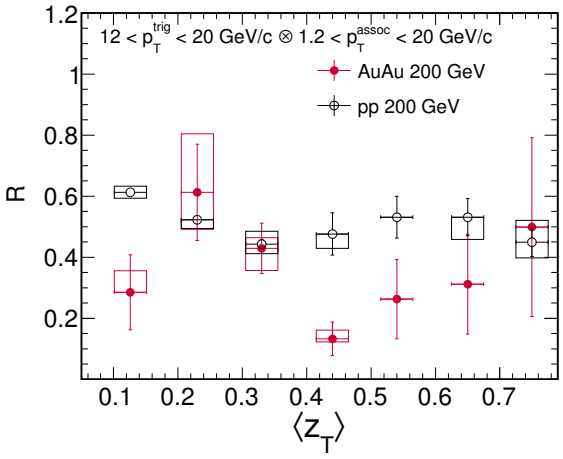

Figure 16: The values of R both for pp and AuAu (0-12%) for different z_T bins.

The trigger dependence for R values is shown in Fig. 17.

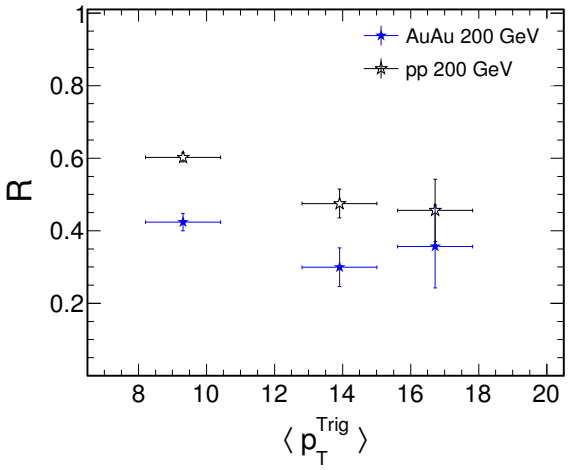

Figure 17: The values of R both for pp and AuAu (0-12%) at $0.3 < z_T < 0.6$ bins.

0.8.2 study of purity check for π^0 and γ^{dir}

If we apply no PID cuts for the "gamma-rich" sample (and the π^0 is a subset of the "gamma-rich", then on the near-side

$$Y^{\gamma_{rich}} = \frac{N^{\gamma_{rich}+h}}{N^{\gamma_{rich}}} \quad (8)$$

$$= \frac{N^{\pi^0_{sym}+h} + N^{\gamma_{decay}+h}}{N^{\pi^0_{sym}} + N^{\gamma_{decay}} + N^{\gamma_{direct}}}. \quad (9)$$

Here π^0_{sym} are symmetrically decaying π^0, for which the calorimeter cluster energy is the energy of the full π^0, while γ_{decay} are the single photons from asymmetric π^0 decays and those from η decays. We assume that the correlation function for symmetric pi^0 is the same as that for decay-photon triggers. (This was previously checked to be a reasonable assumption with PYTHIA.) Then the yield measured with our nearly-pure sample of π^0 triggers

$$Y^{\pi^0} = \frac{N^{\pi^0_{rich}+h}}{N^{\pi^0_{rich}}} \quad (10)$$

$$= \frac{N^{\pi^0_{sym}+h} + N^{\gamma_{decay}+h}}{N^{\pi^0_{sym}} + N^{\gamma_{decay}}}. \quad (11)$$

is equal to the yield of all "background" triggers.

Now, calculating the ratio R, using the near-side yields,

$$R = \frac{Y^{\gamma_{rich}}}{Y^{\pi^0}} \quad (12)$$

$$= \frac{N^{bgd}}{N^{\gamma_{rich}}} \quad (13)$$

$$= \frac{N^{\pi^0_{sym}} + N^{\gamma_{decay}}}{N^{\pi^0_{sym}} + N^{\gamma_{decay}} + N^{\gamma_{direct}}} \quad (14)$$

$$= \frac{1}{1 + \frac{N^{\gamma_{direct}}}{N^{\pi^0_{sym}} + N^{\gamma_{decay}}}}. \quad (15)$$

We need to relate the ratio $\frac{N^{\gamma_{direct}}}{N^{\pi^0_{sym}} + N^{\gamma_{decay}}}$ to the experimentally measured ratio of γ/π^0. Since this is just decay kinematics, we ran a simple Monte Carlo to simulate π^0 and η decays. We defined "symmetric" π^0 as those with opening angle smaller than the size of one tower. The symmetric π^0 were recorded as a function of the pi^0 p_T, since we measure the cluster energy to be that of the two decay photons together. For the pi^0 that do not pass this criterion and for all η decays, the p_T of the decay photon is recorded. The η is scaled by the measured η/π^0 ratio of 0.4, and the additional factor of 0.39 for the branching ratio to two photons. Then the ratio of $\frac{N^{\pi^0_{sym}} + N^{\gamma_{decay}}}{N^{\pi^0}}$ is calculated as a function of p_T from the sum of Figs. 18 and 19.

Since the ratio γ/π^0 is measured by PHENIX (shown in Figs. 20 and 21), we can compare $\frac{1}{1+\gamma/(1.02\pi^0)}$ to our R. This assumes that the reconstruction efficiency for π^0 and γ is the same for the STAR analysis. This is approximately true except for the charged-rejection cut, which can have a larger effect on a wider cluster. Based on the percent of γ vs. π^0 triggers rejected, this is only a 3% effect. So finally we compare our measured R with the quantity $\frac{1}{1+1.03\gamma/(1.02\pi^0)}$, where γ/π^0 is from PHENIX, in the Fig 22.

In absence of embedding samples of single photons and $\pi^0 \to \gamma\gamma$ in Run-11 Au+Au and Run-9 p+p, we did a quick study of the transverse shower profile with what was available to us. We took a smaple of embedded π^0 Dalitz decays ($\pi^0 \to \gamma e^+ e^-$) and looked at single decay photons (those which hit a tower not hit by the other decay products) and compared to triggers where the full π^0 hit one tower. Figure 23 shows the comparison of clusters where

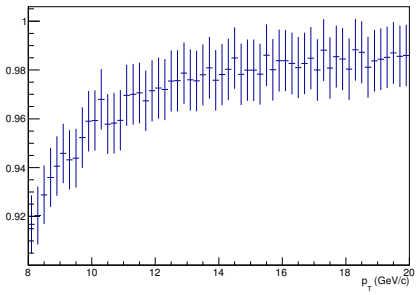

Figure 18: Ratio of symmetric π^0 plus photons from asymmetric pi^0 decays divided by the total number of π^0 as a function of reconstructed p_T.

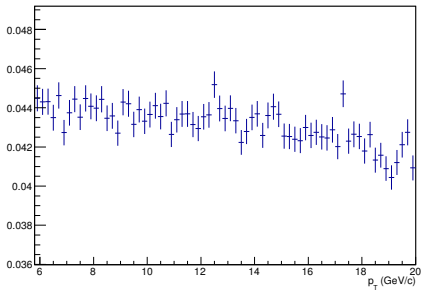

Figure 19: Ratio of photons from η decays divided by the number of π^0 as a function of reconstructed p_T.

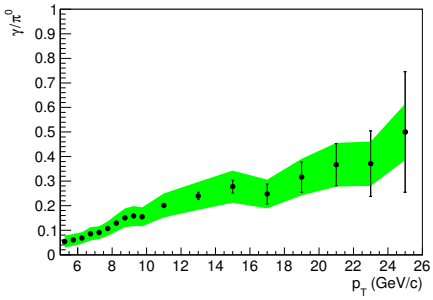

Figure 20: Ratio of direct photon to π^0 cross section measured by PHENIX in p+p collisions.

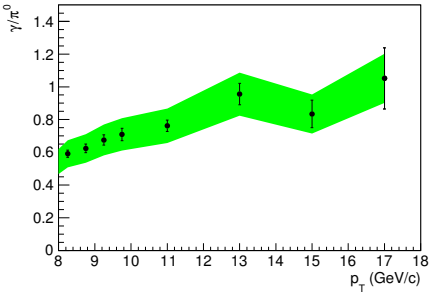

Figure 21: Ratio of direct photon to π^0 cross section measured by PHENIX in 0-10% central Au+Au collisions.

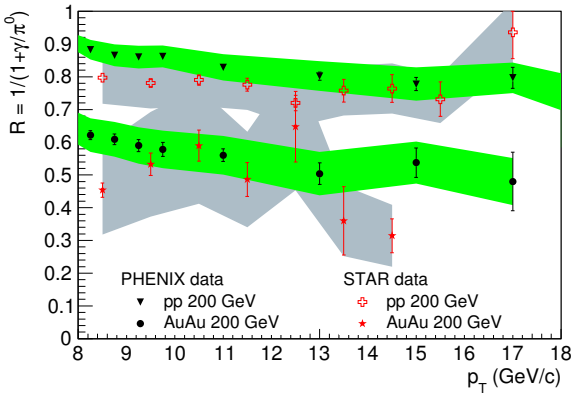

Figure 22: The values $R \sim \frac{1}{1+\gamma/\pi^0}$, obtained from PHENIX experiment for Au+Au central collisions and p+p collisions at 200 GeV, are shown in the black marker with systematic errors (green band). Values of R obtained from this analysis (STAR experiment) for Au+Au (central colliisions) and p+p collisions at 200 GeV, are shown in red markers. The gray bands are systematic uncertainties on the ratio R.

a single photon vs. the full π^0 hits one tower, for cluster energies $8-20$ GeV. The average cluster energy from this sample is ~ 13 GeV. The wider clusters (π^0) have a TSP distribution at lower values than the more narrow single-photon clusters. Addressing the question of well well the TSP can separate single photons from π^0 at higher energies, we looked at the same comparison for cluster energies $16-20$ GeV (where the mean was ~ 18 GeV) in Fig. 24. Here both the single photon and the π^0 TSP distributions shift to higher values (narrower showers), but the ratio within the cut region (TSP<0.08) is approximately the same.

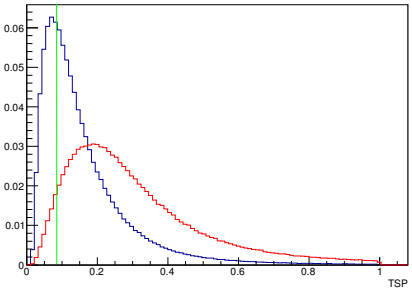

Figure 23: Transverse Shower Profile quantity (TSP) for average cluster energy of ~ 13 GeV for single photons (red) vs. full π^0 (blue) hitting one tower. The green line indicates the cut to select π^0 in data.

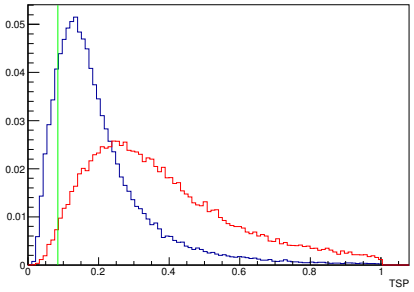

Figure 24: Transverse Shower Profile quantity (TSP) for average cluster energy of ~ 18 GeV for single photons (red) vs. full π^0 (blue) hitting one tower. The green line indicates the cut to select π^0 in data.

We can also compare the TSP distributions from embedding to data. Here we allow a combination of the TSP distributions (from a single photon, photon plus one electron or positron, and photon plus both electron and position (full π^0) hitting one tower) to make up the TSP distrbution observed in Au+Au data. The comparison is done for triggers with an average cluster energy of 11.3 GeV, both for data and embedding, although the energy distributions are different. This average cluster energy is what is in the output of the data from the Level-2 Gamma algorithm. We allow for both 2 particles and 3 partiv=cles to hit one tower because both have a disadvantage. The 3-particle towers are a little bit wider than the 2-particle towers, but the 2-partcle towers come from higher energy π^0 than in the data (where we measure $\pi^0 \to \gamma\gamma$). Figure 25 shows the comparison. The 3-particle clusters (green) are a bit wider (smaller TSP values) than the 2-particle clusters (magenta), and both are significantly different from the single-photon clusters (blue). Their amplitudes were allowed to vary in a fit to the data (red). In this (somewhat rough) study, the single photon clusters make up $\sim 7\%$ of the data for TSP<0.08, based on the fit.

Finally, Fig 26 shows the fragmentation functions as a function of z_T, for π^0 trigger and charged hadron trigger [3] are same for AuAu collisions.

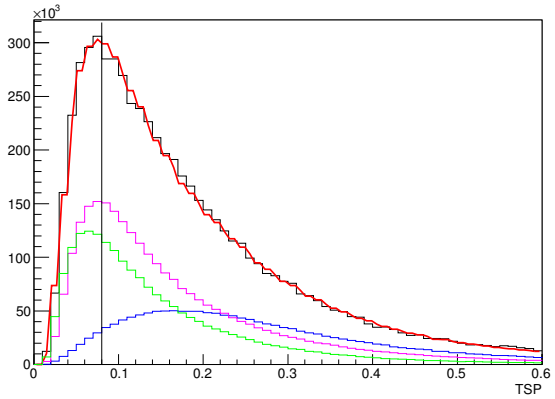

Figure 25: The TSP distribution of trigger candidates in Au+Au data (black histogram) compared to single photons (blue), two-particle clusters (magenta) and 3-particle clusters (green). The red is a fit to the data with the individual contributions as shown.

Comparison of new and published results

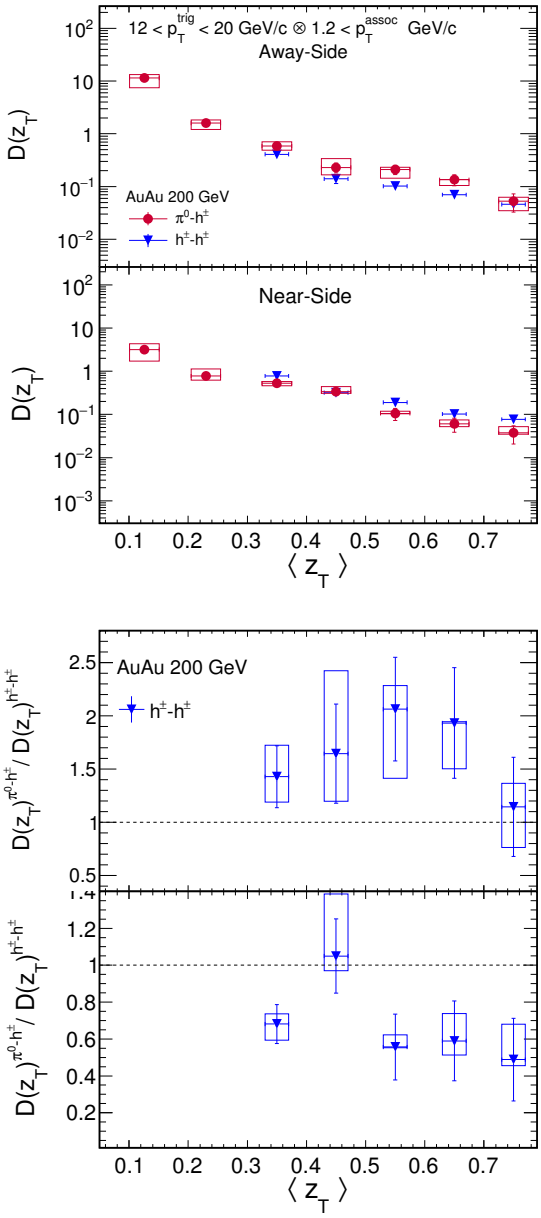

Figure 26: The comparison of charged hadron fragmentation functions [3] and that for π^0 hadron trigger both for near-side and away-side.

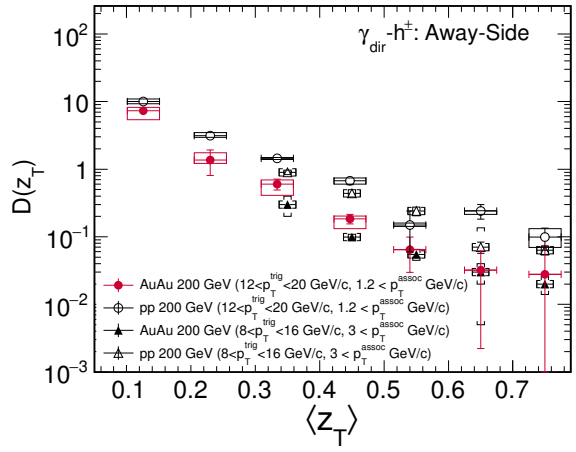

Figure 27: Comparison of FF at different kinematic range for γ^{dir} trigger.

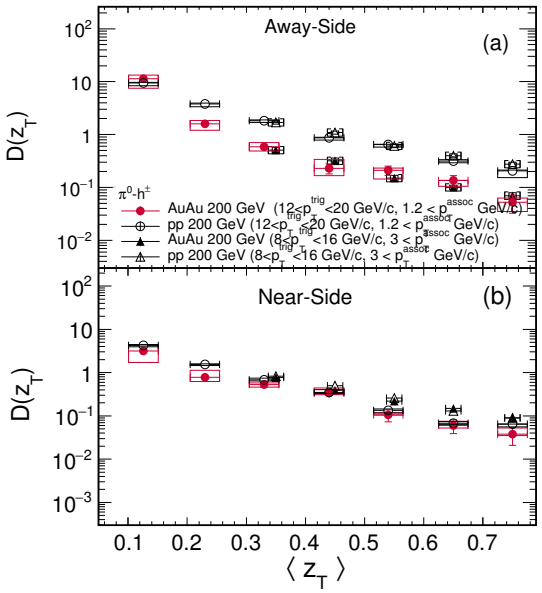

Figure 28: Comparison of FF at different kinematic range is for π^0 trigger.

Comparison of pp results to PYTHIA

We can also compare our results for π^0-triggered and direct-photon-triggered yields in p+p collisions to PYTHIA. Figures 30-**??** show the ratio of PYTHIA to data of near-side yields for π^0 triggers, away-side yields for π^0 triggers, and away-side yields for direct γ triggers, respectively.

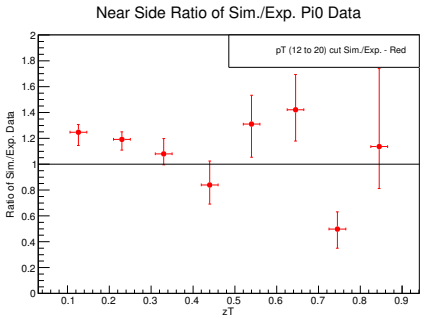

Figure 29: Comparison of near-side yields for π^0 triggers.

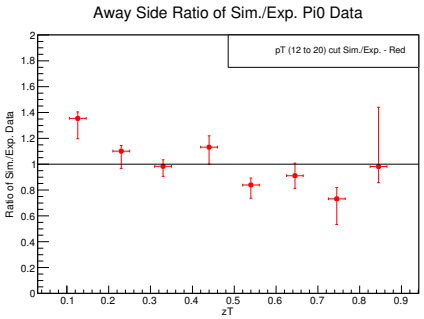

Figure 30: Comparison of away-side yields for π^0 triggers.

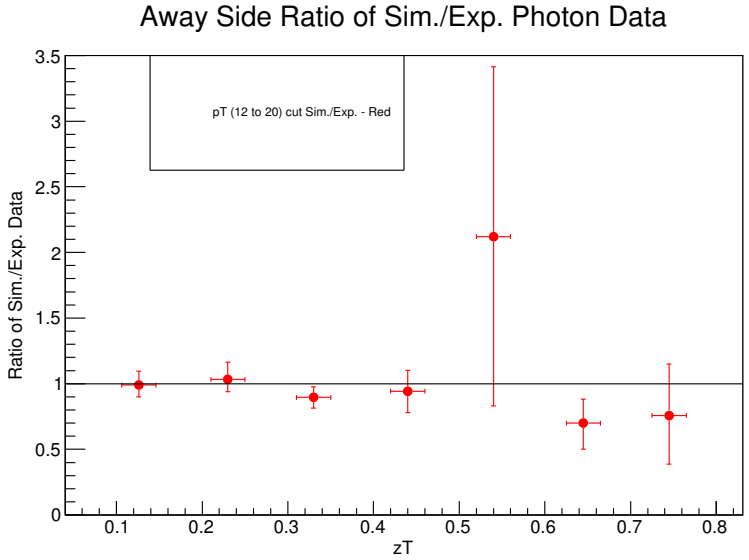

Figure 31: Comparison of FF for direct photon triggers

The agreement between data and PYTHIA is reasonable (within $\sim 20-30\%$). It is noteworthy that the direct photon triggers in PYTHIA do not include fragmentation photons. In data, we have subtracted this as part of our background with the assumption that the correlation function for a fragmentation photon is the same as for a π^0.

0.9 Statistical and Systematic error estimation

Statistical error estimation

Mainly, statistical errors of the various spectra are estimated by using root histograms. Whereas, yields of away-side hadrons of γ^{dir} trigger depend on the $Y^a_{\gamma_{rich}+h}$, $Y^a_{\pi^0+h}$ and R, as follows,

$$Y_{\gamma_{dir}+h} = \frac{Y^a_{\gamma_{rich}+h} - RY^a_{\pi^0+h}}{1-R} \tag{16}$$

For simplification, above equation can be written as follows

$$Y^{\gamma} = \frac{X^{\gamma} - RX^{\pi}}{1-R} \tag{17}$$

After using error propagation method, one can get variance (stat. error) of the Y^{γ} ($= Y^a_{\gamma_{rich}+h}$)

$$\begin{aligned} Var(Y^{\gamma}) = \frac{1}{(1-R)^2}[Var(X^{\gamma}) + R^2 Var(X^{\pi}) + \\ (\frac{X^{\gamma}-X^{\pi}}{1-R})^2 Var(R) + \\ \frac{2(X^{\gamma}-X^{\pi})}{1-R} Cov(X^{\gamma},R) - \frac{2R(X^{\gamma}-X^{\pi})}{1-R} Cov(X^{\pi},R)] \end{aligned} \tag{18}$$

Systematic error estimation

Systematic error estimation is done based on following method.

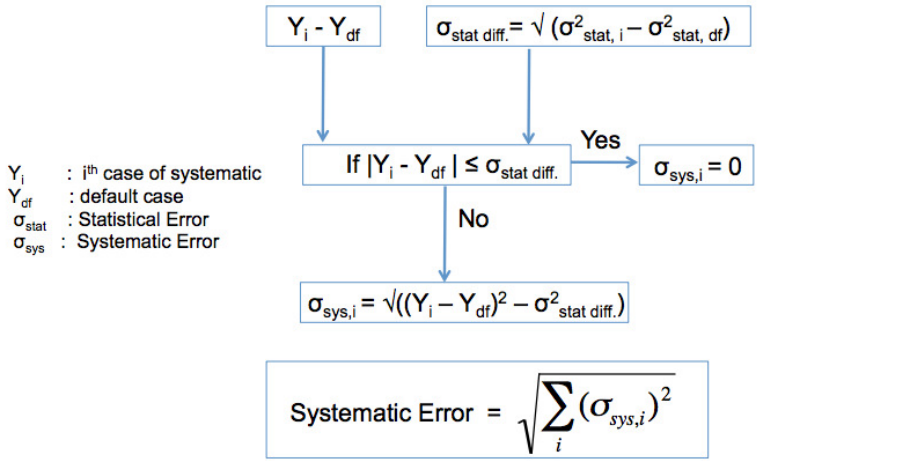

- $\sigma_{sys,i}$ **is the different independent systematic error**
  - **Such as track quality cuts, Y_{rich} and π^0_{rich} samples variation, tower rejection, ZYAM window, etc.**

Various systematic checks are done to understand systematic effect on near and away side hadrons yields both for γ^{dir} and π^0 trigger. In order to remove/minimize statistical fluctuations from systematic uncertainty, we have subtracted stat. error as described in the above flow-chart. Mainly, in this method, we try to separate source of uncorrelated systematic uncertainties and then we add by quadrature all uncorrelated sources. In this list only, maximum contributing sources, from each uncorrelated sample for systematic uncertainty, are taken. Those systematic sources are listed below.

1. DCA < 1 (Default DCA < 3)

2. DCA < 1 and Fit points > 20
3. Fit points > 10
4. Fit points > 20
5. 0.2 < TSP < 0.5 for gamma rich (Default 0.2 < TSP < 0.6)
6. 0.15 < TSP < 0.6 for gamma rich
7. 0.2 < TSP < 0.7 for gamma rich
8. TSP < 0.07 for pi0 rich (Default TSP < 0.08)
9. Removal of towers with projected tracks having p > 2 GeV/c
10. Removal of towers with projected tracks having p > 4 GeV/c
11. ZYAM window [1.0,1.5]
12. Yield window $|\Delta\phi| < 1.1$
13. Yield window NS $|\Delta\phi| < 0.9$ and AS $|\Delta\phi - \pi| < 1.1$
14. systematic on $< v_2 >$

The main contributions for systematic difference from default values come from choice of ZYAM [from above list Sys#11,12] and Yield extraction [Sys#13] windows. The systematic effects of purity and TSP cuts for π^0 and γ^{dir} [Sys#5-8] have also been checked. It is found that their effects varies maximum upto $10-20\%$. Whereas, flow contributions (mainly $< v_2 >$, Sys#14) are very negligible as shown in the following plots and table. In addition to these, 3% uncertainty on efficiency calculation are included in systematic error.

The table for systematic uncertainty can be found below.

zT bin	Sys-1	Sys-2	Sys-3	Sys-4	Sys-5	Sys-6	Sys-7	Sys-8	Sys-9	Sys-10	Sys-11	Sys-12	Sys-13	Sys-14
0.1	-0	-0	0	-0	0.806171	-1.77951	-0	0	0	0	-0	0	-0	0
0.2	0	0	0	0	0	-0	-0	0	0	0	0	-0	0	0
0.3	-0.0246873	-0.0519447	0.0280054	-0.0217895	0.0791435	-0.167965	-0	-0.0718782	-0	-0	-0	-0	-0	-0
0.4	-0.0054844	-0.0313726	0.00619663	-0.0252535	0.0162588	-0.040409	-0.00606437	-0.00412329	-0	-0	0.00587545	0	0.00587545	-0
0.5	0	-0	-0	-0	0	-0	-0	0	-0	-0	0	0	0	-0
0.6	0	0	0	0	0	-0	-0	-0	0	0	0	0	0	0
0.7	0	0	0	0	0	-0	-0	-0	0	0	0	0	0	0
0.8	-0	-0	0	-0	0	-0	-0	-0.00748014	0	0	0	0	0	0

Table 1: Various systematic errors as listed above for γ^{dir} trigger for AuAu collisions.

zT bin	Sys-1	Sys-2	Sys-3	Sys-4	Sys-5	Sys-6	Sys-7	Sys-8	Sys-9	Sys-10	Sys-11	Sys-12	Sys-13	Sys-14
0.1	-1.1376	-3.36517	1.8617	-2.63644	0	0	0	-1.8074	-0.7537	-0.7537	5.898	-1.7716	5.898	-0.1618
0.2	-0.16445	-0.38796	0.24104	-0.36653	0	0	0	0.04863	-0.03899	-0.03899	0.08714	0.02796	0.08714	-0.0176
0.3	-0.00988	-0.062511	0.065144	-0.097743	0	0	0	0.10177	-0.002297	-0.002297	0.052931	0.004217	0.052931	-0.001047
0.4	-0.025062	-0.062656	0.030075	-0.027569	0	0	0	0.104828	-0.001255	-0.001255	0.077647	0.03121	0.077647	-0.001
0.5	-0.040051	-0.062607	0.022556	-0.030075	0	0	0	-0.021889	-0.000448	-0.000448	0.037656	-0.00794	0.037656	-0.000408
0.6	-0.030075	-0.030075	0	0	0	0	0	0.00092	0	0	0	0	0	0
0.7	-0.0150374	-0.0150374	-0.0175845	0	0	0	0	0.0102569	0	0	0	0	0	0
0.8	0	0	0	0	0	0	0	0.0118504	0	0	0	0	0	0

Table 2: Various systematic errors as listed above for π^0 trigger of AS for AuAu collisions.

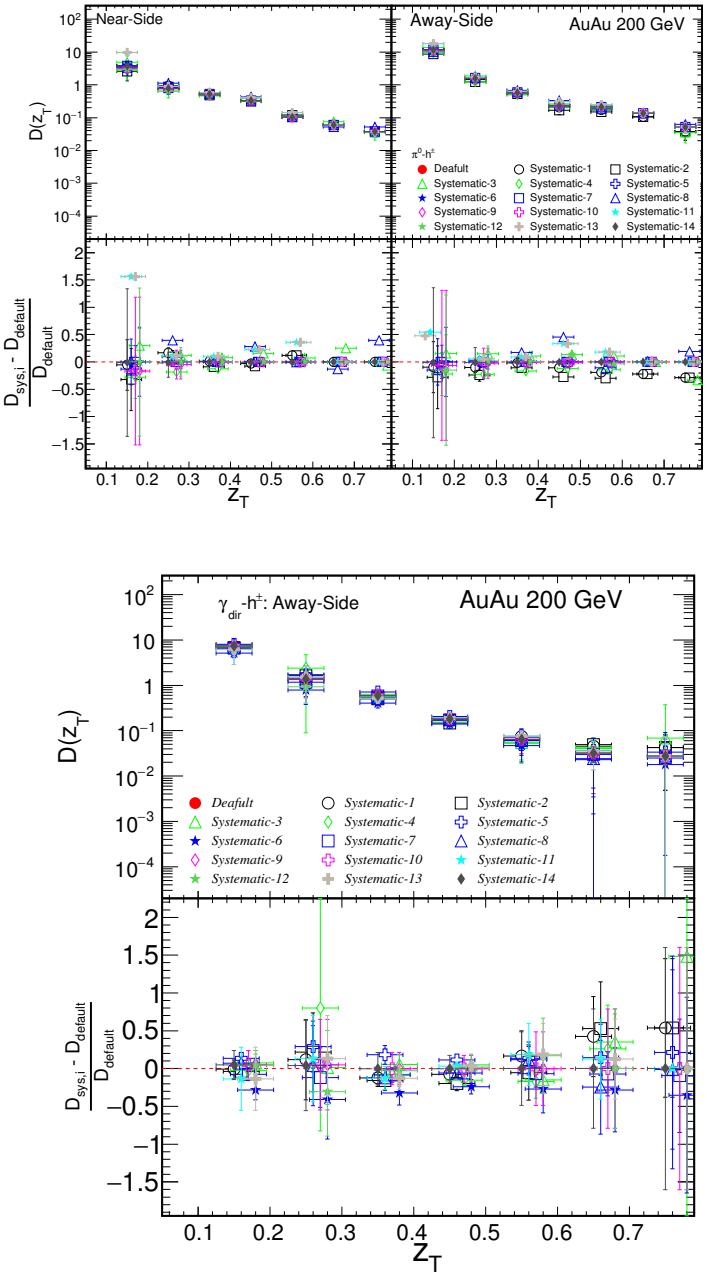

Figure 32: Various systematic effect as listed above are shown here for AuAu collisions.

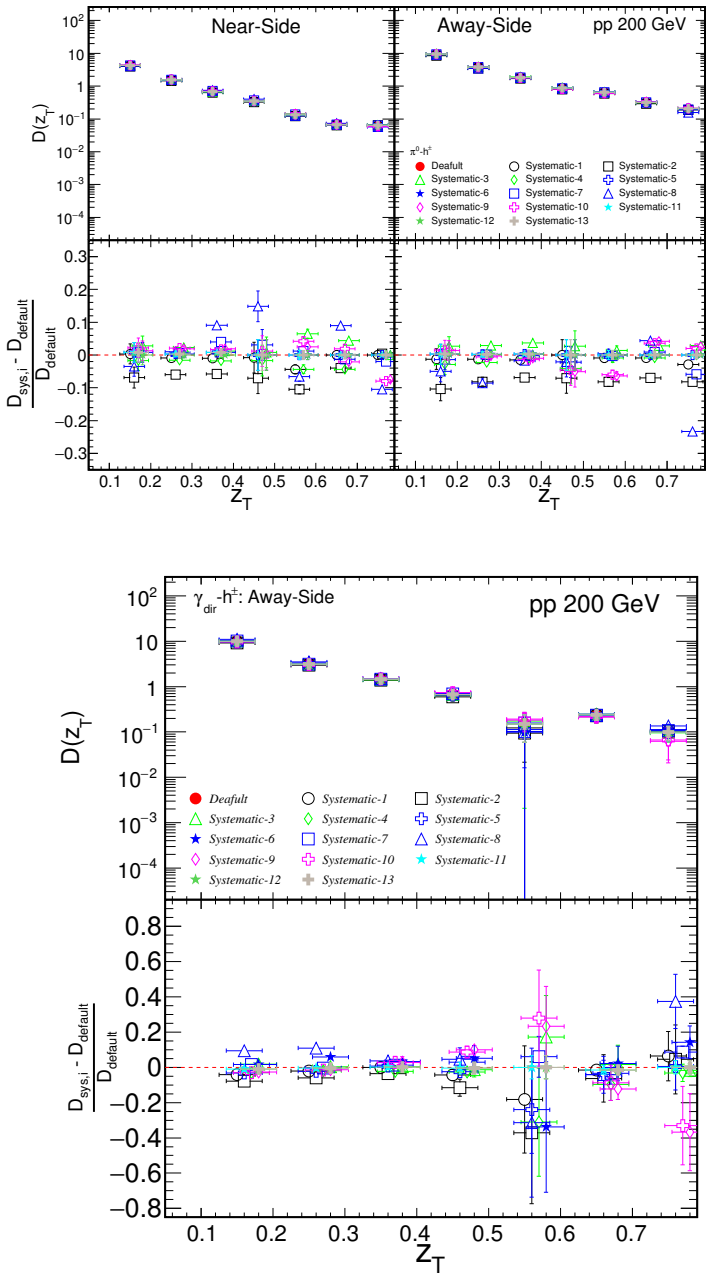

Figure 33: Various systematic effect as listed above are shown here for pp collisions.

zT bin	Sys-1	Sys-2	Sys-3	Sys-4	Sys-5	Sys-6	Sys-7	Sys-8	Sys-9	Sys-10	Sys-11	Sys-12	Sys-13	Sys-14
0.1	-0.20571	-1.22334	1.14044	-1.06278	0	0	0	-0.48673	-0.63164	-0.63164	5.90083	-0.84163	5.90083	-0.03559
0.2	0.136566	0.078547	0.098104	-0.148379	0	0	0	0.315603	-0.03726	-0.03726	0.087156	-0.165945	0.087156	-0.015729
0.3	0.005265	-0.047366	0.042574	-0.067669	0	0	0	0.007629	-0.001697	-0.001697	0.052972	-0.00271	0.052972	-0.000438
0.4	-0.010063	-0.0251	0.052631	-0.005031	0	0	0	0.093811	-0.001499	-0.001499	0.077564	-0.014148	0.077564	-0.001243
0.5	0.012561	0.012561	0.007519	0	0	0	0	-0.000466	-0.000476	-0.000476	0.037636	-0.000449	0.037636	-0.000436
0.6	0	0	0.0150374	0	0	0	0	-0.0077432	0	0	0	0	0	0
0.7	0	0	-0.0025234	0	0	0	0	0.014813	0	0	0	0	0	0
0.8	0	0	0	0	0	0	0	0.0013691	0	0	0	0	0	0

Table 3: Various systematic errors as listed above for π^0 trigger of NS for AuAu collisions.

zT bin	Sys-1	Sys-2	Sys-3	Sys-4	Sys-5	Sys-6	Sys-7	Sys-8	Sys-9	Sys-10	Sys-11	Sys-12	Sys-13
0.1	-0.387378	-0.758911	0.153057	-0.266679	-0.279833	0.049171	0.101531	0.926648	-0.233512	-0.273114	-0	-0	-0
0.2	-0.026717	-0.169678	0	-0.0363195	-0.0322534	0.179432	-0	0.336728	-0	-0	-0	-0	-0
0.3	0	-0.0476902	0	-0.0283624	0	0.0412856	0	0.0291925	0	0	0	0	0
0.4	-0.0197935	-0.0711945	-0	-0	-0.00750413	0	0.00942318	0	0.0644306	0.0545948	-0	-0	-0
0.5	-0	-0	0	-0.00761055	-0	-0	0	-0	0.00708768	0.0091495	0	0	0
0.6	-0	-0	0	-0.00762676	-0	0	-0	-0	-0.026317	-0	-0	-0	-0
0.7	0	0	-0	-0	0	0.0106511	0.00786333	0.0336361	-0.029111	-0.0241565	0	0	0
0.8	0	0	-0	0	0	-0	0	0	0	0	0	0	0

Table 4: Various systematic errors as listed above for γ^{dir} trigger for pp collisions.

zT bin	Sys-1	Sys-2	Sys-3	Sys-4	Sys-5	Sys-6	Sys-7	Sys-8	Sys-9	Sys-10	Sys-11	Sys-12	Sys-13
0.1	-0.11811	-0.98422	0.25008	-0.26883	0.02516	0.02516	-0.13363	-0.47265	0.13188	0.14533	0.02516	0.02516	0.02516
0.2	-0.04871	-0.30981	0.111	-0.0888	0.00774	0.00774	0.00256	-0.32676	-0.01177	-0.02275	0.00774	0.00774	0.00774
0.3	-0.02709	-0.12523	0.06653	-0.01831	0.00509	0.00509	-0.00339	-0.03051	-0.01754	-0.02559	0.00509	0.00509	0.00509
0.4	0	-0.06097	0.023404	-0.035106	0	0	-0.018918	-0.017697	-0.044302	-0.040022	0	0	0
0.5	-0.005851	-0.053085	0.008777	-0.005851	0	0	-0.002128	0.002744	-0.041277	-0.038778	0	0	0
0.6	-0.002926	-0.022167	0.008776	-0.002926	0	0	0.002928	0.013921	0.013332	0.0113	0	0	0
0.7	-0.005851	-0.016761	0.005851	0	0	0	-0.012127	-0.047701	0.005331	0.004034	0	0	0
0.8	0.021942	0.013722	0.033644	0.021942	0.021942	0.021942	0.017707	0.007185	0.016368	0.015536	0.021942	0.021942	0.021942

Table 5: Various systematic errors as listed above for π^0 trigger AS for pp collisions.

zT bin	Sys-1	Sys-2	Sys-3	Sys-4	Sys-5	Sys-6	Sys-7	Sys-8	Sys-9	Sys-10	Sys-11	Sys-12	Sys-13
0.1	0.01354	-0.29231	0.11843	-0.0699	0.03393	0.03393	0.03263	-0.14887	0.05564	0.09229	0.03393	0.03393	0.03393
0.2	-0.0136	-0.09315	0.03494	-0.02444	0.00482	0.00482	0.00894	0.01531	0.02953	0.03223	0.00482	0.00482	0.00482
0.3	-0.006607	-0.039021	0.008021	-0.012458	0.005095	0.005095	0.026928	0.061516	0.012614	0.011468	0.005095	0.005095	0.005095
0.4	-0.002926	-0.024956	0.002925	-0.005851	0	0	0.011004	0.052122	0.000178	0.004244	0	0	0
0.5	-0.005851	-0.01412	0.008776	-0.005851	0	0	0.001616	-0.008906	0.003413	0.005678	0	0	0
0.6	0	-0.0026533	0.0029255	-0.0029255	0	0	-0.0008528	0.0060192	-0.0014293	0.001281	0	0	0
0.7	0	0.0002722	0	0	0	0	-0.001249	-0.0067637	-0.004776	-0.0051437	0	0	0
0.8	0.0029255	8.67e-05	0.0029255	0.0029255	0.0029255	0.0029255	0.0060951	0.0057022	0.00461	0.0044552	0.0029255	0.0029255	0.0029255

Table 6: Various systematic errors as listed above for π^0 trigger NS for pp collisions.

0.10 Results

We comapre $I_{AA}^{\gamma^{dir}}$ as a function of z_T for AuAu collisions with that of the theoretical model predictions by G.-Y. Qin *et al.* [8] and X. N. Wang *et al.* [9, 10, 11]. In this theoretical model, the direct photon-hadron correlations calculation are done using energy loss of hard jets by employing a fully (3+1)-dimensional hydrodynamical evolution model. In Fig. **??**, $I_{AA}^{\gamma^{dir}}$ shows nice agreement with that of G.-Y. Qin *et al.* and X. N. Wang *et al.* model prediction. In Fig **??**, $I_{AA}^{\gamma^{dir}}$ are plotted as function of average p_T^{assoc}, and the above model predictions are compared as well. It shows the suppression of away side hadron of tagged γ^{dir} are in well agreement with G.-Y. Qin *et al.* model prediction.

Fig.39 shows NS associated hadron yields for p+p collisions as a function z_T. this red line represent the exponential fit function as mentioned in the plot. Different dotted lines represent systematic variation of fitting parameter's error.

$$f(z_T) = e^{(a-bz_T)} \tag{19}$$

where a and b are the fitting parameters as mentioned in the Fig 39.

$$I = \int_0^1 z_T e^{(a-bz_T)} dz_T \tag{20}$$

$$frac.\ contribution = \frac{1}{1+I} \tag{21}$$

By integrating NS yield of associated hadron of π^0 trigger, it is found that $83\% - 88\%$ of energy carried by pi0 trigger over total parton energy.

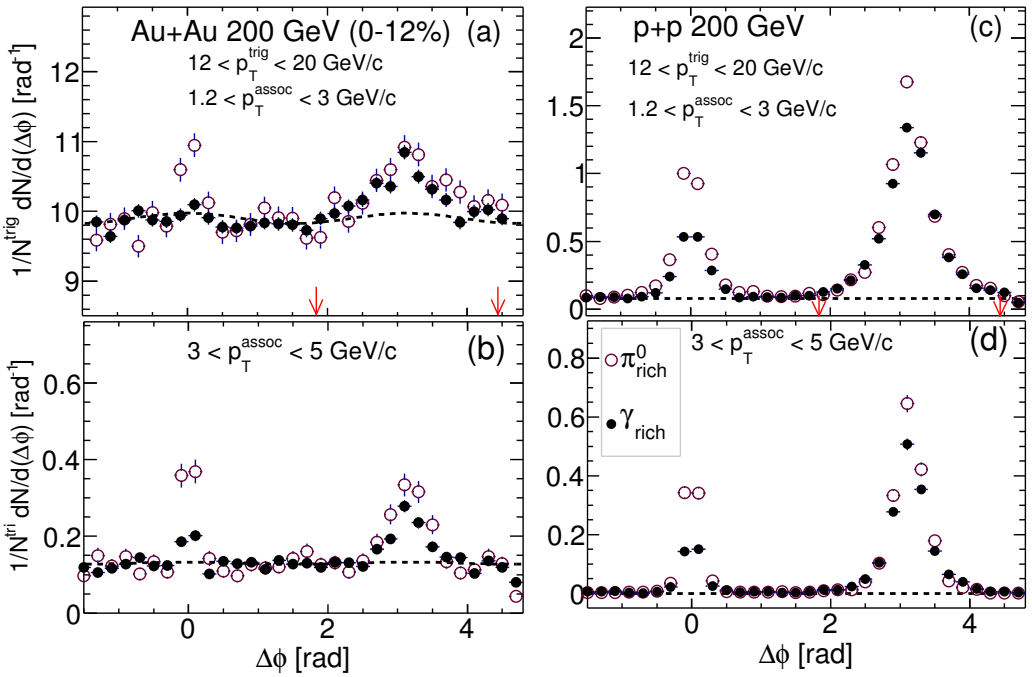

Figure 34: Correlation functions for triggered π^0_{rich} and γ_{rich} samples with associated charged hadrons measured in central (0-12%) AuAu collisions and pp collisions.

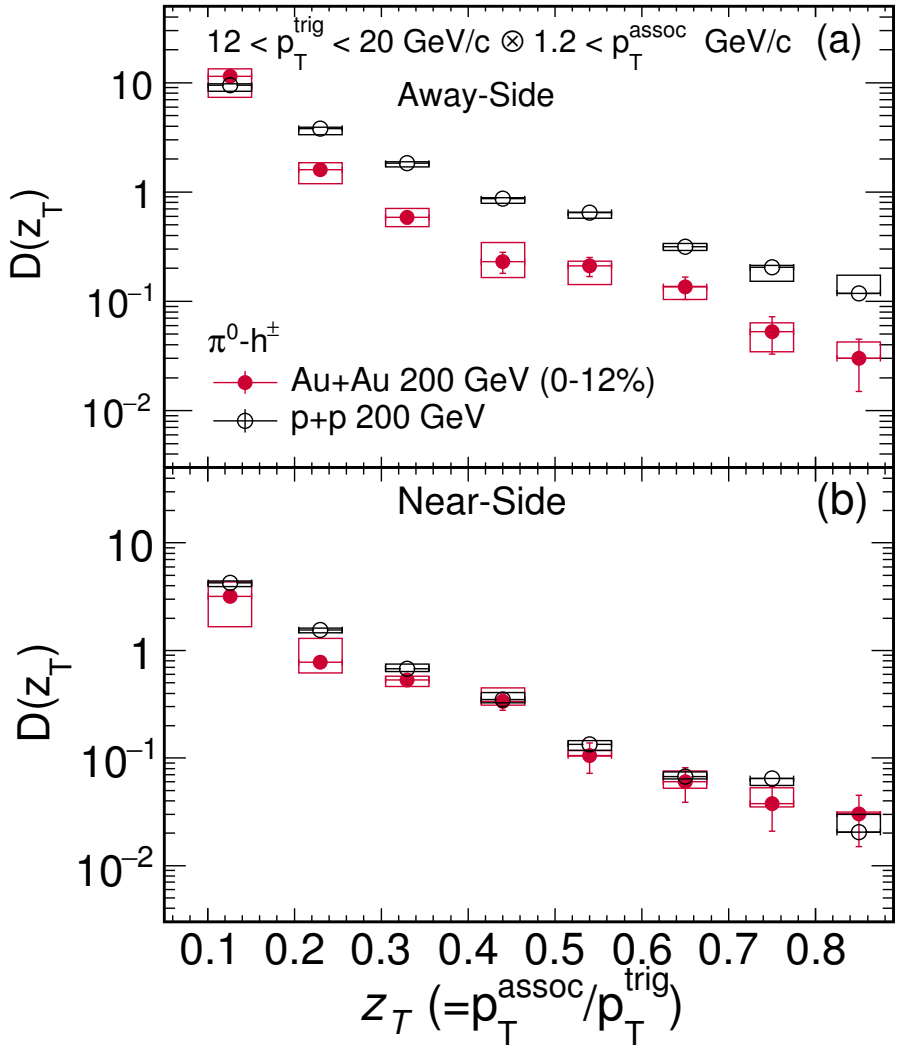

Figure 35: The z_T dependence of $\pi^0 - h^{\pm}$ away-side associated particle yield for AuAu at 0-12% centrality and pp collisions.

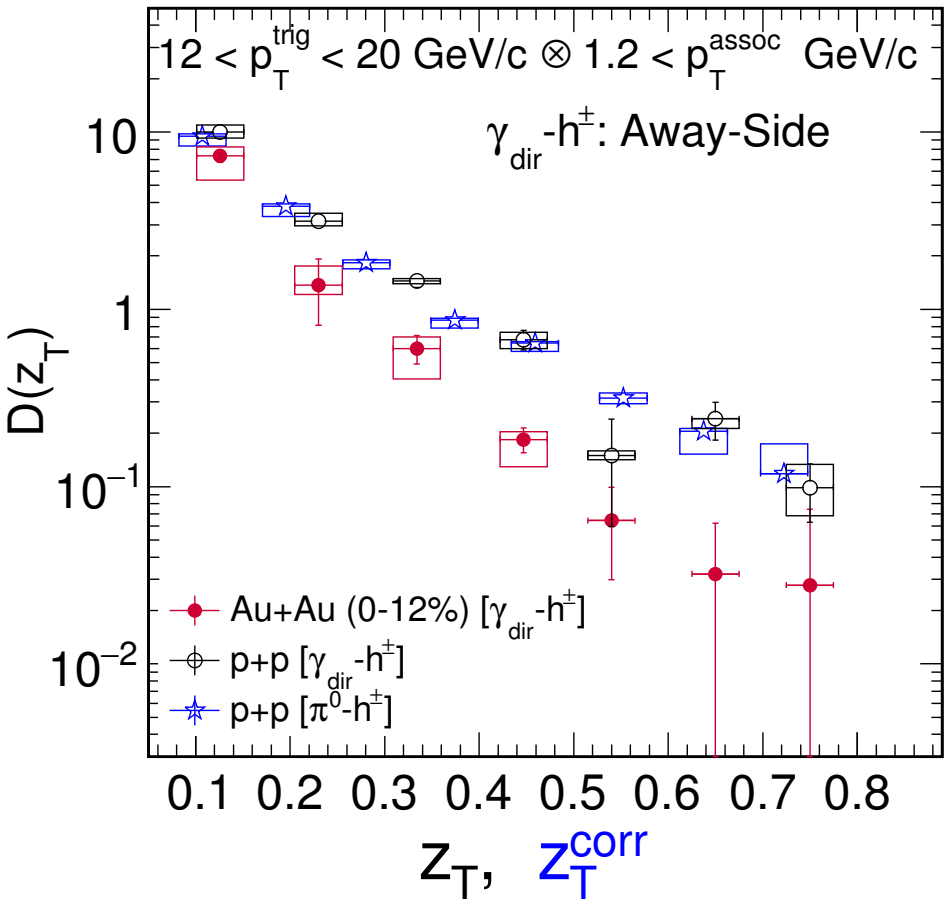

Figure 36: The z_T dependence of γ^{dir}-$h^{\pm}$ away-side associated particle yield for AuAu at 0-12% centrality and pp collisions.

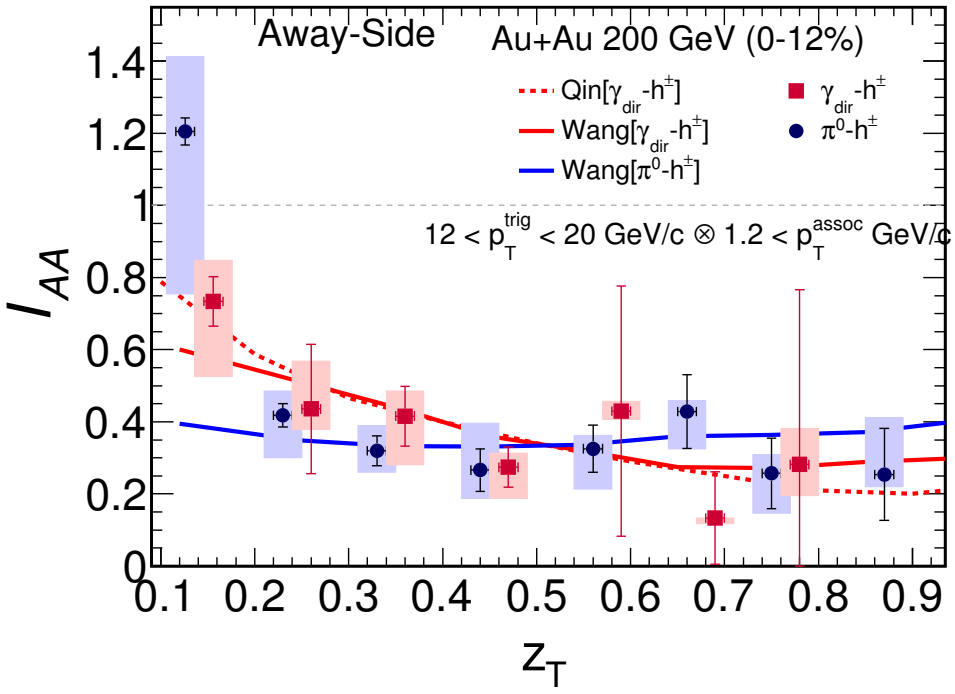

Figure 37: The z_T dependence of π^0-$h^{\pm}$ away-side (upper panel) and near- side (lower panel) associated particle yield for AuAu at 0-12% centrality and pp collisions.

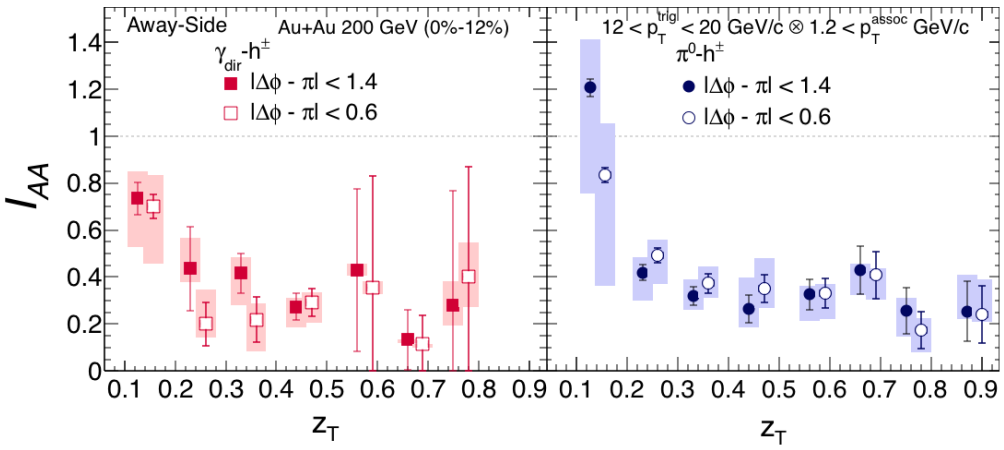

Figure 38: I_{AA} as a function of z_T for different $|\Delta\phi - \pi|$ integration window for triggered π^0_{rich} and γ_{dir} hadron correlations.

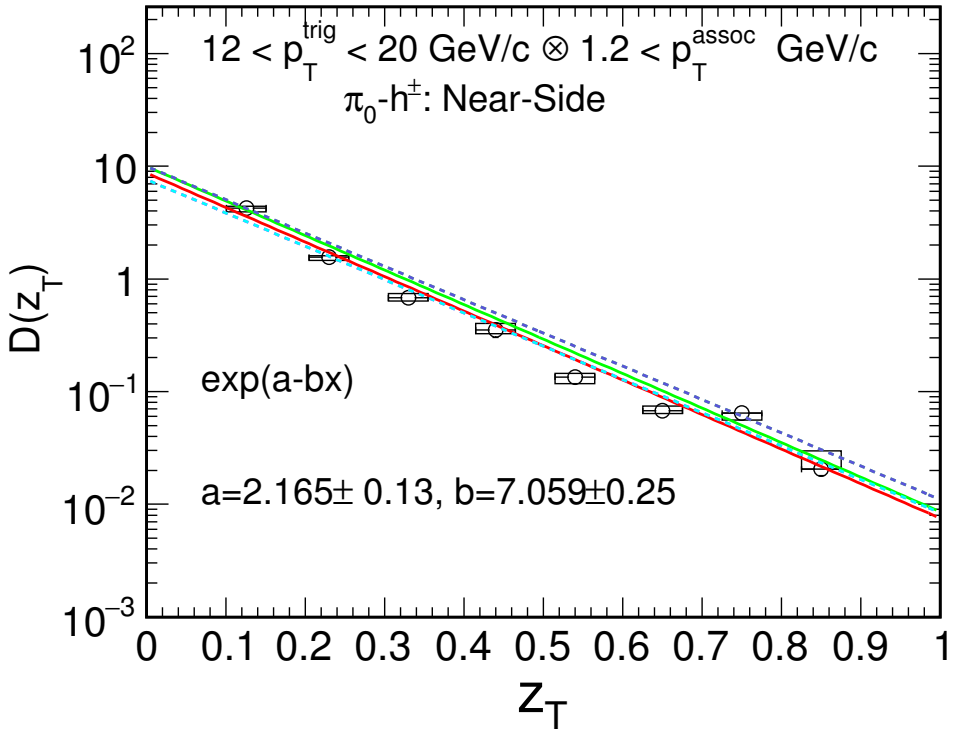

Figure 39: Same as lower panel Fig.35 for p+p collisions, The red line represents the exponential fit function as mentioned in the plot. Different dotted lines represent systematic variation of fitting parameter's error. By integrating NS yield of associated hadron of π^0 trigger, it is found that $83\% - 88\%$ of energy carried by pi0 trigger over total parton energy.

Bibliography

[1] N. Wang, Z. Huang, and I. Sarcevic, Phys. Rev. Lett. 77, 231 (1996).

[2] B. I. Abelev et al., (STAR Collaboration) Phys. Rev. C **82**, 034909 (2010).

[3] J. Adams et al., (STAR Collaboration) Phys. Rev. Lette. **97**, 162301 (2006).

[4] http://www.star.bnl.gov/protected/common/common2011/trigger2011/streams.html

[5] http://www.star.bnl.gov/protected/common/common2009/trigger2009/triggers2009.html#200GeV

[6] http://www.star.bnl.gov/protected/jetcorr/hamed/Direct_photon_link/Direct_photon_link/Online_trigger.html

[7] http://www.star.bnl.gov/protected/jetcorr/nihar/2014Jun10_JetCorr_Nihar.pdf

[8] G.-Y Qin *et al.*, Phys. Rev. C **80**, 054909 (2009).

[9] X. F. Chen, T. Hirano, E. Wang, X. N. Wang and H. Zhang, Phys. Rev. C **84**, 034902 (2011).

[10] X. F. Chen, C. Greiner, E. Wang, X. N. Wang and Z. Xu, Phys. Rev. C **81**, 064908 (2010)

[11] H. Zhang, J. F. Owens, E. Wang and X. N. Wang, Phys. Rev. Lett. **103**, 032302 (2009), H. Zhang, J. F. Owens, E. Wang and X. N. Wang, Phys. Rev. Lett. **98**, 212301 (2007)